USGS
science for a changing world

EXPLANATORY NOTES FOR THE MINERAL-RESOURCES MAP OF THE CIRCUM-PACIFIC REGION NORTHWEST QUADRANT

1:10,000,000

To Accompany Map CP-46

CIRCUM-PACIFIC COUNCIL
FOR
ENERGY AND MINERAL
RESOURCES

1999

U.S. Department of the Interior
U.S. Geological Survey

CIRCUM-PACIFIC COUNCIL FOR ENERGY AND MINERAL RESOURCES
Michel T. Halbouty, Founder

CIRCUM-PACIFIC MAP PROJECT
John A. Reinemund, Director
George Gryc, General Chair

EXPLANATORY NOTES FOR THE MINERAL-RESOURCES MAP OF THE CIRCUM-PACIFIC REGION NORTHWEST QUADRANT

By

LAND RESOURCES

Masaharu Kamitani and **Sadahisa Sudo**, Geological Survey of Japan, Higashi 1-1-3, Tsukuba, Ibaraki 305, Japan

Yoshihiko Shimazaki, Nikko Exploration and Development Co., Ltd., Toranomon 2-7-10, Minatoku, Tokyo 105, Japan

Tomoyuki Moritani, Sumitomo Construction Co., Ltd., Arakicho 13-4, Shinjukuku, Tokyo 160-8577, Japan

George Gryc, U.S. Geological Survey, Menlo Park, California 94025, U.S.A.

SEAFLOOR RESOURCES

David Z. Piper, Theresa R. Swint-Iki, and **Gretchen Luepke**, U.S. Geological Survey, Menlo Park, California 94025, U.S.A.

Floyd W. McCoy, Windward College, University of Hawaii, Kaneohe, Hawaii 96744, U.S.A.

Frank T. Manheim and **Candice Lane-Bostwick**, U.S. Geological Survey, Woods Hole, Massachusetts 02543, U.S.A.

1999

Explanatory Notes to Supplement the

MINERAL-RESOURCES MAP OF THE CIRCUM-PACIFIC REGION NORTHWEST QUADRANT

Tomoyuki Moritani, Chair
Northwest Quadrant Panel

Compilers and Principal Contributors*

LAND RESOURCES

Masaharu Kamitani, Geological Survey of Japan, Tsukuba, Ibaraki 305-8567, Japan
Pow Foong Fan, Hawaii Institute of Geophysics, Honolulu, Hawaii 96822, USA
Keiichiro Kanehira, Chiba University, Yayoi 1-33, Chiba, 260, Japan
Shunso Ishihara, Geological Survey of Japan, Tsukuba, Ibaraki 305-8567, Japan
Yoshihiko Shimazaki, Geological Survey of Japan, Tsukuba, Ibaraki 305-8567, Japan
Katherina Radkevich, Far East Geological Institute, Vladivostok 690022, Russia
W. David Palfreyman, Australian Geological Survey Organisation, Canberra, A.C.T. 2601, Australia
Sadahisa Sudo, Geological Survey of Japan, Tsukuba, Ibaraki 305-8567, Japan

SEAFLOOR RESOURCES

David Z. Piper, U.S. Geological Survey,Menlo Park, California 94025, USA
Theresa R. Swint-Iki, U.S. Geological Survey, Menlo Park, California 94025, USA
Floyd W. McCoy, University of Hawaii, Kaneohe, Hawaii, USA
Frank T. Manheim, U.S. Geological Survey, Woods Hole, Massachusetts 02543, USA
Candice M. Lane-Bostwick, U.S. Geological Survey,Woods Hole, Massachusetts 02543, USA
Lawrence G. Sullivan, Lamont-Doherty Earth Observatory, Palisades, New York 10964, USA
Atsuyuki Mizuno, Geological Survey of Japan, Tsukuba, Ibaraki 305-8567, Japan
Gretchen Luepke, U.S. Geological Survey, Menlo Park, California 94025, USA

*Affiliations are at time of compilation

Compilation coordinated by
George Gryc
U.S. Geological Survey
Menlo Park, California 94025, USA

CONTENTS

INTRODUCTION

CIRCUM-PACIFIC MAP PROJECT

By
George Gryc , U.S. Geological Survey
and
Tomoyuki Moritani, Sumitomo Construction Co., Ltd.

The Circum-Pacific Map Project (CPMP) is a cooperative international effort designed to show the relationship of known energy and mineral resources to the major geologic features of the Pacific Basin and surrounding continental areas. Available geologic, mineral-resource, and energy-resource data are being integrated with new project-developed data sets such as magnetic lineations, seafloor mineral deposits, and seafloor sediment. Earth scientists representing 180 organizations from more than 40 Pacific-region countries are involved in this work.

Six overlapping equal-area regional maps at a scale of 1:10,000,000 form the cartographic base for the project: the four Circum-Pacific quadrants (northwest, southwest, southeast, and northeast) and the Antarctic and Arctic regions. There is also a Pacific Basin Sheet at a scale of 1:17,000,000. The published map series include the base (published from 1977 to 1989), the geographic (published from 1977 to 1990), the plate-tectonic (published from 1981 to 1992), and the geodynamic (published from 1984 to 1990) maps; all of them include seven map sheets. The thematic map series in the process of completing publication include Geologic (publication initiated in 1983), Tectonic (publication initiated in 1991), Energy-Resources (publication initiated in 1986), and Mineral-Resources (publication initiated in 1984) maps. Altogether, 57 map sheets are planned. The maps are prepared cooperatively by the Circum-Pacific Council for Energy and Mineral Resources and the U.S. Geological Survey. Maps published prior to mid-1990 are available from Dr. H. Gary Greene, Circum-Pacific Council for Energy and Mineral Resources, Moss Landing Marine Laboratory, MLML, Box 450, Moss Landing, California 95039-0450, U.S.A.; maps published from mid-1990 to present are available from the U.S. Geological Survey, Information Services, Box 25286, Federal Center, Denver, CO 80225, U.S.A.

The Circum-Pacific Map Project is organized under six panels of geoscientists representing national earth-science organizations, universities, and natural-resource companies. The regional panels correspond to the basic map areas. Current panel chairs are Tomoyuki Moritani (northwest quadrant), R. W. Johnson (southwest quadrant), Ian W. D. Dalziel (Antarctic region), vacant (southeast quadrant), Kenneth J. Drummond (northeast quadrant), and George W. Moore (Arctic region). Jose Corvalán D., chaired the Southeast Quadrant Panel from its inception in 1974 to his death in 1996; the Panel completed compilations of all eight topical maps of that quadrant.

Project coordination and final cartography are being carried out through the cooperation of the U.S. Geological Survey under the direction of Map Project General Chair George Gryc of Menlo Park, California. Project headquarters are located at 345 Middlefield Road, MS 952, Menlo Park, California 94025, U.S.A. The project has been overseen from its inception by John A. Reinemund, director of the project since 1982.

The framework for the Circum-Pacific Map Project was developed in 1973 by a specially convened group of 12 North American geoscientists meeting in California. Philip W. Guild, deceased, was one of the original group of scientists who developed the framework of the Circum-Pacific maps and was largely responsible for the format and explanatory symbols for the mineral resource series. The project was officially launched at the First Circum-Pacific Conference on Energy and Mineral Resources held in Honolulu, Hawaii, in August 1974. Sponsors of the conference were the American Association of Petroleum Geologists (AAPG), Pacific Science Association (PSA), and the Committee for Coordination of Joint Prospecting for Mineral Resources in Asian Offshore Areas (CCOP). The Circum-Pacific Map Project operates as an activity of the Circum-Pacific Council for Energy and Mineral Resources, a nonprofit organization that promotes cooperation among Circum-Pacific countries in the study of energy and mineral resources of the Pacific basin. Founded by Michel T. Halbouty in 1972, the Council also sponsors quadrennial conferences, topical symposia, scientific training seminars, and the Earth Science Series of publications.

Published thematic maps of the Northwest Quadrant include the Plate-Tectonic Map (Nishiwaki, 1981; revised by Inoue, 1987), the Geodynamic Map (Nishiwaki, 1985), the Geologic Map (Inoue, 1988), and the Energy-Resources Map (Sumii and others, 1992). The Tectonic Map is now in cartographic preparation at CPMP headquarters in Menlo Park, California.

MINERAL RESOURCES MAP OF THE NORTHWEST QUADRANT

By
Masaharu Kamitani , Geological Survey of Japan,
Tomoyuki Moritani, Sumitomo Construction Co., Ltd.,
and
George Gryc, U.S. Geological Survey

The Mineral-Resources Map of the Circum-Pacific Region Northwest Quadrant is the fifth published in a series of six overlapping 1:10,000,000-scale mineral-resources maps. The Mineral-Resources Map of the Circum-Pacific

Region Northeast Quadrant (Drummond) was published in 1985, the Mineral-Resources Map of the Circum-Pacific Region Southeast Quadrant (Corvalán and others), and Mineral-Resources Map of the Circum-Pacific Region Southwest Quadrant (Palfreyman and others) were published in 1996, and the Mineral-Resources Map of the Circum-Pacific Region Antarctic Sheet (Guild, Piper, and others) was published in 1998.

The Mineral-Resources Map series is designed to be as factual as possible, with a minimum of interpretation. The small scale, 100 km/cm or 10,000 km^2/cm^2 (about 160 miles per inch or 25,000 square miles per square inch), requires an enormous simplification of both the background information and the mineral-deposit data; hence, the maps can only give a general impression of the distribution, character, and geologic environment of these resources. Nevertheless, this map series provides a unified overview of the mineral resources of a region encompassing more than half the globe. It should identify areas broadly favorable for the occurrence of specific minerals and assist both in resource assessment and, with additional data from more detailed sources, in exploration planning. The maps also serve to show the relation of deposits to major earth features, such as divergent and convergent plate margins, hotspots, and accreted terranes, and should stimulate analysis of the role of geologic processes in the genesis of ores.

The maps show both land and seafloor deposits of most metallic and nonmetallic minerals, except for construction materials. Uranium and thorium are included, although their principal use is for energy production. Deposits on land are shown regardless of their status of exploration, and some deposits may have been totally exhausted. The maps do not, therefore, necessarily represent the present resource picture. In general, only deposits of economic size and grade are shown, but some small or low-grade occurrences have been included, where space permits, in order to indicate a resource potential. Deposits on land are shown by colored symbols outlined in black that are explained in detail on the maps.

Because most seafloor deposits have not been evaluated for their economic potential, the criterion for their inclusion on the maps is simply knowledge of their existence. Reported occurrences of nearshore heavy minerals (placer deposits) are indicated by chemical symbols (letters) in blue.

Offshore mineral resources depicted are: (1) manganese-iron oxide nodules that contain varying amounts of nickel, copper, and cobalt, and trace amounts of other metals; (2) sulfide deposits; and (3) phosphatic deposits. No attempt has been made to show the distribution of metalliferous sediments which are known to be widespread but are so low in grade that they are not considered to be resources at the present time (Field and others, 1981).

Mineral-resource information for the land and nearshore areas is assembled by members of the individual quadrant panels; compilers, contributors, and data sources are cited on the maps themselves. Information on the offshore resources has been assembled for the entire ocean area of the project principally by geologists of the U.S. Geological Survey.

The geologic background for the Mineral-Resources Maps are taken from the corresponding geologic maps, but are in general simplified and in part modified to emphasize features that may be significant in explaining the distribution of the mineral deposits. Almost all of the principal mineral deposits in this quadrant are related to granitoids. Although the project aims at a uniform presentation throughout the Circum-Pacific region, differences among the compilers in interpretation of its geologic evolution may result in some variation in the representation of the background information of land areas from map to map. For this Northwest Quadrant Map the geologic background was compiled from both the corresponding Energy-Resources Map (Sumii and others, 1992) and the corresponding Geologic Map (Inoue and others, 1988). Color is used to denote the structural state and depositional environment of the stratified rocks. Igneous intrusive and extrusive rocks are differentiated by color, and gray patterns differentiate felsic, mafic, or alkaline composition of the igneous rocks. A description of the background geology for the Energy Resources map of the Northwest Quadrant by Wakita and Sumii, 1992, from which the background geology for this map was compiled for: crystalline basement rocks, metamorphic complexes, intrusive igneous rocks, volcanic rocks, continental-margin rocks of Late Proterozoic and Phanerozoic Age is as follows:

Crystalline Basement Rocks. The rocks classified as basement rocks are Precambrian in age include marine sedimentary rocks, metamorphic rocks, felsic intrusive and extrusive rocks, ultramafic to mafic intrusive rocks, and anorthosite.

Intrusive Igneous Rocks. Intrusive igneous rocks range in age from Paleozoic to Tertary, and in composition from gabbro to granite. Most ages of major batholiths are Mesozoic to Paleogene.

Metamorphic Complexes. The areas shown as metamorphic include a variety of rocks ranging in age from Late Proterozoic to Tertiary that are highly deformed, metamorphosed, and in places intruded by granitic rocks. They range from greenschist facies up to gneiss. Some of them have metamorphic affinity with the ancient accretionary complexes.

Volcanic Rocks. Paleozoic to Quaternary volcanic rocks, ranging in composition from basalt to rhyolite, are widely distributed in the Northwest Quadrant area. Major distribution of Quaternary volcanic rocks is parallel to the present trench systems. Large amounts of felsic extrusive igneous rocks of Cretaceous to Paleogene age are extensively distributed along the continental margin of East Asia.

Continental-Margin Rocks of Late Proterozoic and Phanerozoic Age. Continental-margin rocks include two types of rocks: ancient accretionary complexes characterized by the occurrence of melange, and covered sedimentary sequences on platforms which were deformed by later tectonism. The ancient accretionary complexes consist of sedimentary and slightly metamorphosed rocks, including melange, turbidites, fragments of microcontinents, and remnant island arecs that are found along existing continental margins, on island arcs, and between ancient continental blocks. These complexes have been intensely deformed by faulting and folding. The covered sedimentary rocks are distributed on the margins of ancient continental blocks such as the Siberian, North China, and Yangtze Platforms. The platform deposits consist of nonmarine and marine sediments which are folded to various degrees.

On this mineral-resources map, however, platform deposits and basin and margin deposits have been shown as separate units from the accretionary complexes of the continental-margin rocks.

Quaternary continental and marine sedimentary deposits, ultramafic rocks, lithology, and geologic contacts, faults, and ages are from the Geologic Map of the Circum-Pacific Region, Northwest Quadrant (Inoue and others, 1988).

Mineral distribution is shown according to the main metal or mineral content, type, age, and size of individual deposit.

Compilation of this map involved contributions from many individuals and organizations. Philip W. Guild, as advisor to the Mineral-Resources Map series since the inception of the project, took the lead in the selection of the map elements, units, and symbols, especially for land resources. David Z. Piper and Theresa R. Swint-Iki did most of the compilation and analysis of seafloor mineral data. Australian mineral deposit data were compiled from a number of (mainly published) geologic and metalliferous maps of various scales produced by the Australian Geological Survey Organisation (AGSO) and by State and Territory government geoscience organizations.

The Mineral-Resources Map of the Northwest Quadrant was prepared under the direction of the present panel chair Tomoyuki Moritani and the previous panel chair Eiji Inoue, both formerly of the Geological Survey of Japan.

The final compilation of the map was coordinated by Masaharu Kamitani and Shunso Ishihara, Geological Survey of Japan, and Yoshihiko Shimazaki, formerly of the Geological Survey of Japan, with the assistance and advice of past and present Northwest Quadrant panel members and the staff of the Geological Survey of Japan, notably Chikao Nishiwaki and Keiichiro Kanehira. The contributions of Katherine Radkevich and Warren J. Nokleberg for the mineral deposit data and map of the Russian territories and W. David Palfreyman for the mineral map of the southern Pacific area are acknowledged with appreciation.

The Northwest Quadrant Panel is composed of the following members: Tomoyuki Moritani (Chair), Yuji Endo, Keizo Fujii, Jiro Hirayama, Eiichi Honza, Masaharu Kamitani, Osamu Matsubayashi, Masao Nakanishi, Hiro'o Natori, Tamotsu Nozawa, Tadashi Sato, Yoshihiko Shimazaki, Sadahisa Sudo, Tomoaki Sumii, Kensaku Tamaki, Yoji Teraoka, Koji Wakita, and Takashi Yoshida, Japan; Kim Dong Hak and Hyen-II Choi, Korea; Raymundo S. Punongbayan, Philippines; Tran Van Tri, Le Van Cu, and Nguyen Khac Vinh, Vietnam; Sivavong Changkasiri and Saengathit Chuaviroj, Thailand; Yin Ee Heng and Khoo Hang Peng, Malaysia; H.M.S. Hartono, M. Untung, and Tohap Simanjuntak, Indonesia; Greg Anderson and Stevie Nion, Papua, New Guinea; and Maurice J. Terman and Frank F. H. Wang, U.S.A.

RESOURCE SYMBOLS

By

Masaharu Kamitani, Geological Survey of Japan
David Z. Piper and Theresa R. Swint-Iki, U.S. Geological Survey

Because mineral resources vary widely in their characteristics, the symbols that represent the deposits have been designed to impart as much information as possible at the map scale. Although the map explanations give the details, a brief discussion of the system may be helpful to the reader.

LAND RESOURCES

The legend for the land mineral resources has been modified and simplified from the Preliminary Metallogenic Map of North America (North American Metallogenic Map Committee, 1981) and described by Guild (1981). The map symbols show the metal or mineral content of the deposits by colored geometric shapes. The colors, insofar as possible, show metals or minerals of similar type: copper and associated metals are orange, precious metals are yellow, and lead-zinc and associated minerals are blue. The 5 shapes and 10 colors indicated on the legend of the map provide 50 combinations, but not all of them have been used here.

Three sizes of symbols denote the relative importance of the deposits. Limits between the size categories for each commodity are, for the most part, in terms of metric tons of the substance(s) contained before exploration. These limits are obviously arbitrary; they have been selected on the basis of the worldwide abundance of the commodity concerned in deposits that are exploitable under current economic and technological conditions.

An exception was made, however, for deposit size discrimination of gold-silver in the Siberia Platform in Russia, because the mineral-deposit data contributed by E.A. Radkevich in 1987 and other published data do not indicate deposit size.

Some deposits shown as small on this map correspond only to occurrences; they have been included because they may help to identify areas broadly favorable for exploration planning of specific minerals.

One or more ticks on the symbol indicate the general nature of the deposit–magmatic, vein, stratabound, laterite, and placer. Most of the eight types are distinctive, but the category designated "stockworks, including porphyry deposits" encompasses such disparate types as sulfur in the cap rock of salt domes, manto deposits, and porphyry deposits, so that judgment must be used in interpreting this symbol. The ticks have been omitted on many of the small symbols either because of ignorance of deposit type or because it was felt unnecessary to identify all of them where they occur in clusters of deposits of the same kind. A description of the eight deposit types shown on the Northwest Quadrant follow:

Veins and shear-zone fillings. Crosscutting, epigenetic deposits in any type of host rock. The major dimensions are transverse to stratification in sedimentary or volcanic hosts. Most stockworks fit here; some in igneous hosts are better equated with the irregular disseminated deposits.

Stratabound, including magmatic cumulates. Deposits, generally of limited horizontal extent, that occur at more or less the same horizon in stratified rocks. May be partly concordant, partly discordant with enclosing rocks. Usually considered to be epigenetic. Examples: carbonate-hosted (Mississippi Valley) lead-zinc deposits, uranium deposits of Colorado Plateau, Wyoming Basin, and so forth. Magmatic cumulates are concordant in layered, generally mafic or ultramafic igneous rocks. Examples: stratiform chromite, ilmenite, platinum-group metals of Bushveld type; and certain nickel-sulfide (komatiite-hosted) deposits.

Stockworks, including "porphyry" deposits. Irregular disseminated deposits, in or associated with intrusive igneous rocks. Parts of some have been described as stockworks. Hydrothermal alteration, including greisenization, common.

Magmatic and irregular massive deposits; includes pegmatites. Examples: podiform chromite, some magnetite and magnetite-ilmenite deposits.

Skarn deposits. Contact-metamorphic (tactite) deposits. Stratified, usually carbonate, rocks intruded by intermediate to acid igneous rock.

Sandstone (red bed) deposits

Laterite deposits (surficial chemical concentrations). Includes laterite, bauxite, uraniferous calcrete, and some manganese oxide deposits. The criterion is that supergene processes were responsible for producing ore-grade material.

Placer deposits (surficial mechanical concentrations). Includes "fossil" black sands.

Mineralization ages for some deposits are indicated by double ticks placed according to a clockwise order from older to younger. Where a tick indicating the deposit type already occurs, a single tick for age is added and the two must be read together. On the Northwest Quadrant map, the age of mineral categories has been changed from the Northeast and Southwest Quadrants, and in the overlap area between the Northwest and Southwest maps, the position of the age ticks has been changed to reflect the different categories on the respective maps.

Space limitations do not permit identifying by name all the deposits shown on the map, but many of the larger ones are named and listed in table 1 with commodity type and latitude/longitude.

SEAFLOOR RESOURCES

The potential value of manganese nodules depends on their abundance and composition. Abundance data have been derived principally from seafloor photographs, typical examples of which are reproduced in the explanation on the map. Nodules cover from 0 to nearly 100 percent of the seafloor areas. On the map, squares 2 mm on a side, empty to totally filled in black, indicate where bottom photographs have been taken and the abundance of nodules at these points. Additional information on the occurrence of nodules was gained from core sampling; small black x's and o's indicate where nodules have been recovered or not recovered, respectively, in cores. Details of the methods used in studying these data sources and in deriving abundance contours are described later.

The composition of analyzed nodules is indicated within certain limits by different colored +'s for ranges of nickel plus copper content and by brown +'s with chemical symbols for those with high manganese or high cobalt. Areas of nodules averaging 1.8 percent or more nickel plus copper (considered as potentially exploitable—McKelvey and others, 1979) are outlined in red. Composition of analyzed manganese crusts is indicated by colored asterisks for four ranges of cobalt content (Manheim and Lane-Bostwick, 1989).

The polymetallic sulfide deposits thus far discovered on the spreading ridges are shown by black semicircles. Occurrences of sulfides found in Deep Sea Drilling Project

(DSDP) and Ocean Drilling Project (ODP) cores, which may have originated at a ridge and moved off it since their formation, are shown by smaller semicircles and identified by the DSDP or ODP site number.

Submarine hot springs not related to spreading, which in a few near-shore locations are known to be precipitating metallic minerals (though not in economic quantities), are shown by open semicircles.

Seafloor phosphorite occurrences are depicted by brown horizontal lozenges without an outline. Although this symbol is approximately as large as that used for the medium-sized land deposit, it has no size or grade significance. The many guano-type phosphate deposits on oceanic islands so small that the symbol obscures them entirely are distinguished by having a black outline and the tick indicating a surficial chemical concentration.

Bathymetry and the nature of surficial sediment constitute the background for the oceanic areas. The 4 types of surficial sediment shown are simplified from the 13 categories shown in the Geologic Map series. Active plate boundaries are taken from the Plate-Tectonic Map, but spreading axes are depicted as lines of uniform width rather than by varying widths reflecting spreading rates.

LAND RESOURCES

by
Masaharu Kamitani and Sadahisa Sudo, Geological Survey of Japan
and
Yoshihiko Shimazaki, Nikko Exploration and Development Co., Ltd.

PRECAMBRIAN BASEMENT

Crystalline basement bodies consisting of Precambrian sedimentary and metamorphic rocks, mafic to felsic intrusive and extrusive rocks, and alkaline and ultramafic rocks occur on the Eurasian continent (fig. 1). The principal basement bodies–the Siberian, North China, Tarim, Yangtze, and Kontum Platforms and the Kolyma Massif–constitute the main framework of the geologic structure of this continent (fig.1). The Siberian Platform, with the largest areal extent, contains two shields: Aldan and Anabar. On the Aldan Shield, the core of granulite facies has a K/Ar age of about 3,400 Ma (Li and others, 1982). On the North China Platform, which extends to the Korean peninsula, granulite-facies metamorphic rocks yielding Rb/Sr ages ranging from 3,430 to 3,670 Ma are unconformably covered by various Late Archean and Late Proterozoic metamorphic rocks (Li and others, 1982). At the Tarim Massif, Late Archean to Middle Proterozoic gneisses and metamorphic granite occur only in the peripheral region of the massif (Zhang and others, 1984). Some metamorphic rocks on the Yangtze Platform yield isotopic ages ranging from Early to Middle to Late Proterozoic (Nozawa and others, 1988).

On the North China Platform, banded-iron formations of various sizes, probably Algoma-type deposits, formed in the upper units of the Archean greenstone belt. The banded-iron ore bodies in the Anshan area (table 1) of the North China Platform are intermittently distributed for 14 km in a north-northwest-south-southeast direction and 20 km east-west of Yianqianshan Mine, Anshan, Liaonging province (Chun and others, 1986). Hematite and magnetite are the main constituent minerals, but the grade is generally low in iron and high in silica. The same type of banded-iron deposit occurs within the Precambrian Gyeonggi massif on the Korean peninsula (Park, 1981). Significant manganese and ferruginous iron deposits also formed in the southern and southeastern parts of the Siberian Platform (Radkevich, 1979).

A Udokan sandstone-type copper deposit (table 1) consisting of three principal ore horizons occurs in the Upper Proterozoic shallow-marine sandstone and siltstone on the southern margin of the Siberian Platform (Sokolov and Grigorev, 1977). Although the ore is high grade and huge reserves are estimated, mining development has come to a halt due to severe environmental conditions and lack of infrastructure.

Although felsic and alkalic intrusive rocks are dominant along the southern margin of the Siberian Platform and the northern part of the North China Platform, significant mineralization related to their magmatism has not been verified so far.

The largest rare-earth deposit in the world has been exploited in Inner Mongolia, China, since the late 1960's. Rare earths in the Baiyun Obo (Bayan Obo), China, (table 1) carbonatites are closely associated with hematite-magnetite mineralization in Proterozoic marine sedimentary dolomite (Bai and Yuan, 1985; Drew and others, 1990). The 35 million-ton rare-earth oxide reserves of this deposit (Sun, 1983) constitute approximately 75 percent of total world reserves.

One of the oldest porphyry copper deposits, Zhongtiaoshan, (table 1), located at the southern margin of the North China Platform, was formed in and around meta-quartz monzonite porphyry and has a K/Ar age of 1,900 to 1,800 Ma. Tongchuan-type stratabound hydrothermal copper deposits at the western edge of the Yangtze Platform are structurally controlled by a regional depression, based on the lithologic characteristics of various sedimentary rocks and their diagenesis and regional metamorphism (Guo and others, 1987).

Orthomagmatic cupriferous nickel sulfide deposits at the Jinchuan Mine, China (table 1), mainly occur in two pyroxene peridotite bodies of a northwest-southeast trend-

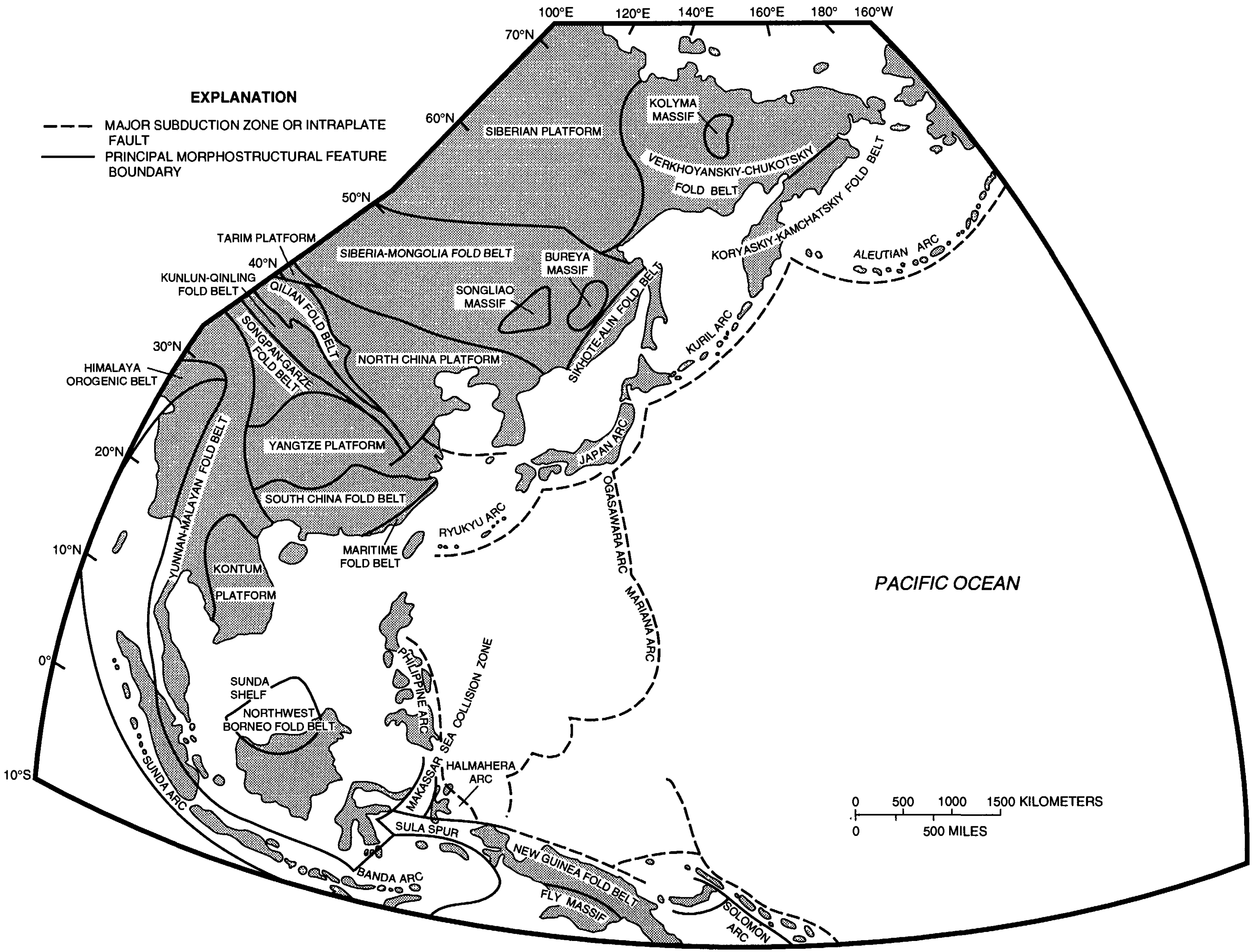

Figure 1.—Index map showing principal morphostructural features of the Northwest Quadrant of the Circum-Pacific region (after Inoue, 1988). Other geographic and structural features included.

ing Proterozoic ultramafic rock complex (Jia, 1986). The ore reserve is estimated at approximately 500 million tons with an average grade of 1.06 percent nickel and 0.67 percent copper and is accompanied by a considerable amount of platinum group elements and cobalt.

Although large vanadiferous uranium deposits have been discovered in the Paleozoic black shale of the Okchon Formation in South Korea, they have not been exploited due to their low-grade ores.

PLATFORM COVER ROCKS OF PHANEROZOIC AGE

Platform cover rocks consisting mainly of marine and continental sedimentary rocks are widely distributed on the Siberian, North China, Yangtze, and Kontum Platforms. These rocks are relatively thin and largely undeformed. Principal mineral resources are evaporite, phosphate, bauxite, stratabound iron and manganese, and sandstone-hosted copper deposits.

Evaporites containing potassium salt extend over the major platforms (Siberian, North China, Yangtze, and Kontum) and they are the host for gypsum and saline minerals. Many evaporites and brine deposits have been explored and exploited along the southern margin of the Siberian Platform, especially along the northeast-trending depression roughly parallel to Lake Baykal, Russia. The thickest Lower Cambrian evaporite contains a thick halite bed, and many lenses of sylvite and carnallite are also preserved (Borchert and Muir, 1964). In China, although evaporites and brines are widely distributed, economically important deposits have been developed mainly in Yunnan Province. One such deposit contains approximately 20 million tons of potassium reserves (Zhang, 1987). Enormous evaporite deposits have been explored by borehole in Thailand in the Khorat Plateau area of the Kontum Platform since the 1960's.

Two evaporite horizons have been verified in Middle to Upper Cretaceous red-bed sequences (Committee for Coordination of Joint Prospecting for Mineral Resources in Asian Offshore Areas (CCOP), 1981; Asnachinda and Pitragool, 1978). The principal mineral is halite with subordinate gypsum, carnallite, and sylvine. One potassium-bearing evaporite deposit is currently being exploited in east Thailand.

The deposition of sedimentary phosphate has been attributed to divergent upwelling, which brings up dominant nutrient seawater along continental margins. Large phosphate deposits formed along the southern margin of the Siberian Platform from the Late Proterozoic to the Late Cambrian. The reserves of the Khubusgul deposit (table 1) in Mongolia are estimated to be over 1,000 million tons, with 20 to 22 percent P_2O_5 (Notholt and Sheldon, 1986). On the North China and Yangtze Platforms many important phosphorite deposits formed during the Late Sinian (Late Proterozoic) and late Cambrian, respectively. Their depositional environments are inferred to have been marginal banks, basins, marginal slopes, and, rarely, shallow-marine basins (Li, 1986; Ye and others, 1984). One of the largest phosphorite deposits in Asia, the Lao Cai deposit (table 1), is located along the southwest side of the Red River in Vietnam. The phosphate rock reserves are estimated to be over 260 million tons with 10 to 36 percent P_2O_5 (Tran and Nguyen, 1986). Large weathered phosphorite deposits formed on karst terrain of Late Proterozoic to Early Cambrian age are characteristic of the Altai and Sayan mountains along the southern margin of the Siberian Platform (Zanin, 1984).

Three types of bauxite deposits are distinguished in the quadrant: (1) laterite-crust, (2) karst-accumulated, and (3) sedimentary-redeposited types (Liu, 1988; Hutchison, 1983). Laterite-crust bauxite deposits are formed by an *in situ* weathering process of alumino-silicate rocks; they comprise most of the world bauxite resources. The Riau archipelago of Indonesia and western Sarawak of Malaysia are the principal areas of laterite-crust bauxite. In the Riau Archipelago, bauxite deposits have developed on top and on gentle slopes of hills as the result of laterization of Triassic shale, phyllite, quartz syenite, and rhyolite (Sigit and others, 1969). Tertiary and Quaternary basalt of the Kontum and Yangtze Platforms and the South China Fold Belt are other sources of this type of bauxite deposit.

Karst-accumulated bauxite deposits are mainly located on karst formed over late Paleozoic carbonate rocks in south China (Liu, 1988). The bauxite deposits occur as lenticular bodies in the shape of Quaternary sinkholes. The Pingguo and Taiping deposits (table 1) of the Zhuang Autonomous region, Guangxi, on the western Yangtze Platform, are representative. Gibbsite, diaspore, and goethite are the principal constituent minerals, unlike the sedimentary-redeposited deposits in north China. On the North China and Yangtze Platforms, bauxite deposits formed in a reductive fresh-water to shallow-marine environment during the Middle Carboniferous (Liu, 1988; Kamitani, 1987). The main ore mineral is diaspore, accompanied by minor amounts of muscovite, kaolinite, and pyrophyllite, and very rarely by iron and manganese minerals. Kaolinite beds also developed in an environment similar to the sedimentary-redeposited bauxites, but they are closely associated with coal beds, and their depositional ages range from Carboniferous to Tertiary.

Sandstone-hosted bedded-copper deposits occur mainly within Cretaceous red-bed sandstone formations on the Yangtze and Kontum Platforms, but economically important deposits have not been discovered so far.

Stratabound lead-zinc deposits occur mainly on the southwestern part of the Yangtze Platform. Some are found in the Fankou (table 1) and Siding areas in Devonian limestone and dolomite beds; others are hosted within shale and sandstone (Wang and others, 1987). Their ^{34}S and Pb isotope ratios may suggest that these carbonate-hosted lead-zinc deposits are similar to Mississippi Valley-type mineralization.

DEFORMED BASINAL (GEOSYNCLINAL) SEDIMENTS OF PHANEROZOIC AGE

Two contrasting geologic and geotectonic areas are found in East and Southeast Asia. The former region is characterized by mostly Precambrian platforms and Paleozoic to Mesozoic fold belts of various scales (Taira and Tashiro, 1987), whereas the latter is characterized by a few comparatively small cratons and fold belts, younger than those of East Asia (Sato, 1981), with the exception of the Kontum Platform. Complicated island-arc systems between the Eurasian and Australian continents are the most characteristic features of the Southeast Asia region. The fold belts are composed of various kinds of basinal sediment: trench-fill, marginal-sea, intracontinental, and so forth. The thick sequences of clastic, carbonate, and siliceous sedimentary and volcanic rocks have been distinctively folded, faulted, uplifted, eroded, and intruded by silicic magma.

Mineral deposits in the deformed basinal sedimentary rocks are either (1) syngenetic or diagenetic or (2) epigenetic. The former deposits are mostly stratabound, whereas the latter are generally discordant and commonly related directly or indirectly to intrusive magmatic activity accompanied by deformation.

SEDIMENT-HOSTED DEPOSITS

Stratabound lead-zinc deposits have formed principally in carbonate-dominant sedimentary rocks which have accreted to the North China and Yangtze Platforms. The Changbu and Lijiagou deposits (table 1) in the Kunlun-Qinling Fold Belt in China formed within a Middle Devonian alternating sequence of clastic and carbonate sedimentary rocks (Yang and Miao, 1986). In the Songpan-Garze Fold Belt, sandstone- and carbonate-hosted stratabound lead-zinc deposits formed in terrestrial sediment during the Jurassic to early Tertiary (Wang and others, 1987). In the other fold belts around the Yangtze Platform (the Ailao Shan-Hoh Xil Shan, Kunlun-Qinling, and South China Fold Belts), the same type of stratabound lead-zinc deposit formed, closely related to carbonate sediments deposited in marginal seas and intercontinental depressions (Liu, 1984).

VOLCANOGENIC MASSIVE SULFIDE DEPOSITS

The volcanogenic massive sulfide deposits, mainly Besshi-type mineralizations, are closely related to oceanic crust. Within the Sambagawa metamorphic belt, southwest Japan, more than 70 cupriferous iron sulfide deposits, intimately associated with highly metamorphosed oceanic basalt and pelitic sediment, extend approximately 1,000 km easterly. Sulfide ore was deposited conformably within upper Paleozoic to Mesozoic volcano-sedimentary sequences and regionally metamorphosed in a high-pressure/low-temperature environment during Jurassic to Cretaceous time (Kanehira, 1970). Besshi-type deposits also occur in the Philippines and northwest China. The Baiyinchang deposit in China, with several orebodies (Liu, 1986a), occurs in the Kunlun-Qinling Fold Belt accreted with the North China and Tarim Platforms during the early and late Paleozoic. The polymetallic orebodies in this belt are conformable with submarine volcano-sedimentary beds that consist mainly of subalkaline, keratophyre and quartz keratophyre tuff and clastic sediment. In the Philippines, Cyprus-type deposits (such as Barlo and other small-sized orebodies) are found at the top of ophiolitic sequences made up of spilitic basalt, pillow lava, and tuffaceous and cherty sediment at several localities throughout the western and eastern flanks of the archipelago (Zanoria and others, 1984).

Kuroko deposits, composed mainly of lead-zinc, copper, and silver and formed within calc-alkalic submarine volcano-sedimentary sequences, are closely related to middle Miocene dacite and rhyolite magmas. Those of the Kosaka, Shakanai, and Hanaoka Mines (table 1) in northeast Japan are representative. The orebodies are always accompanied by gypsum and barite and are surrounded by characteristic hydrothermal alteration halloes: chloritization, sericitization, and kalinization. In the Philippines and Indonesia, the same type of mineralization has been found in Tertiary submarine volcanic terranes. The Bagakai deposits on Samar Island, southeast Philippines, are underlain by dacite-andesite and their pyroclastics, carbonates, and muddy sediment (Zanoria and others, 1984). The ore-mineral assemblage and associated gangue minerals are similar to those of the Kuroko deposits of northeast Japan. Almost all Kuroko-type mineralization has been found in island arcs and depressional stress environments, whereas most porphyry copper deposits are associated with a compressional tectonic setting (Nishiwaki and Uyeda, 1980).

STRATABOUND MANGANESE DEPOSITS

Stratabound manganese and manganese-iron deposits have formed mainly in continental nonvolcanogenic and volcano-sedimentary sequences. Manganese deposits occur at continental margins and basins of Ordovician to Tertiary age (Yue, 1985). On the Yangtze Platform, two subtypes of manganese deposits are recognized. Shallow-marine sedimentary manganese deposits occur principally in the southwestern and western Guangxi Zhuang Autonomous Region, where large deposits of comparatively low-grade ore are intercalated with carbonaceous, siliceous, and muddy sediment. In the Zunyi area (table 1) of the western Yangtze Platform, many bedded manganese orebodies are formed within clayey and silty sediment on Permian limestone that is covered by bituminous shale and coal beds (He, 1985). The occurrence of manganese and coal sediment shows that they probably formed in lagoonal and terrestrial environments.

Stratabound volcanogenic manganese ore is intimately associated with massive and thin-layered chert beds and mafic volcanic rocks. Many small and low-grade manganese and also iron-manganese deposits occur conformably with chert beds, accompanied by mafic submarine volcanic rocks throughout Japan (Watanabe and others, 1970) and in other Paleozoic and Mesozoic fold belts, mainly on the North China and Yangtze Platforms (Yue, 1985).

ULTRAMAFIC ROCKS

The ultramafic rocks, composed of iron and manganese silicates, mainly olivine and pyroxene, represent mantle material brought to the upper crust or large stratiform intrusives formed within the crust. Throughout the Phanerozoic sequences, these rocks are accompanied by ophiolite complexes in accretional fold belts along suture zones at convergent margins and in mafic-ultramafic complexes intruded into stable terranes of continental shield areas.

Numerous ophiolite bodies occur within suture zones and along continental margins and marginal seas of varying geologic age. Ultramafic rocks such as dunite and harzburgite settled out at the bottom of ophiolite complexes and form hosts to podiform chromite orebodies. The deposit size is variable and ranges from one to several million tons, as the deposits at the Acoje and Coto Mines (table 1) in the Paleogene Zambalez ophiolite belt of west Luzon in the Philippines (Philippine Bureau of Mines and Geosciences, 1986). Intermediate-sized podiform-shaped chromite deposits occur in the southwest innerzone of Japan, but the ores are utilized mostly for refractories, due to their high-aluminum and low-chromium composition.

In Southeast Asia, especially in Indonesia and the Philippines, many laterite nickel deposits formed under tropical and subtropical climatic conditions. Consisting mostly of weathered serpentine peridotite, the deposits commonly contain considerable amounts of nickel, ranging from 1,000 to 2,000 parts per million, and are accompanied by a small amount of cobalt. In the laterite soil derived from tropical weathering of ultramafic bodies, nickel is mainly concentrated as garnierite, a secondary silicate mineral found within saprolite zones in weathering crust. Cobalt is concentrated in the upper saprolite and nontronite zones and is very low grade in the ferricrete zone (Golightly, 1981).

The Palawan and Eastern ophiolite belts of the Philippines and east Sulawesi, Halmahera, and Gebe Island of Indonesia are the most productive and promising metallogenic provinces for cobalt-bearing nickel-laterite deposits. A comparatively large nickel-laterite deposit (Tagaung Taung) (table 1) was recently found on the southern edge of the axial ophiolite belt of north Myanmar (Burma) (Schellmann, 1989).

METAMORPHIC COMPLEXES

Many metamorphic complexes are distributed in this quadrant. The large talc-magnesite deposits of the Haicheng-Dashiqiao area of the Liaodong Peninsula, North China Platform, were formed mainly by Proterozoic regional greenschist-amphibolite metamorphism and subsequent repeated thermodynamic events (Zhu and Li, 1986). Several medium-size magnesite deposits, Geomdeog, Hagnam, and Buyeon (table 1), formed in Early to Middle Proterozoic metasediment in northeastern North Korea (Kim and Hwang, 1983).

Principal graphite deposits were formed by regional metamorphism during the Precambrian. Large but low-grade graphite deposits occur in graphite gneiss, schist, and, rarely, granulite, mainly in the North China Platform of northern China and North Korea, and some deposits occur on the Yangtze Platform and South China Fold Belt (Mo and others, 1989).

A considerable number of gold-bearing quartz veins on the North China Platform are believed to be the result of regional metamorphism-stimulated hydrothermal solutions containing gold and silica dissolved from country rocks (Duan and Lu, 1984). Wang (1985), on the other hand, claims that the principal constituents of gold-bearing quartz veins were extracted from Archean volcano-sedimentary basement, deposited, and then reformed by Hercynian (late Paleozoic) and Yanshanian (Mesozoic) magmatism.

INTRUSIVE ROCKS OF PHANEROZOIC AGE

Due to the very complicated geologic history of this quadrant, various intrusive rocks ranging in age from Precambrian to Cenozoic and in composition from gabbro to granite and alkaline rock suites are found throughout the cratons and mobile belts.

Many Archean felsic and alkaline intrusive rocks occur in the central part and along the southern and southeastern margins of the Siberian Platform, and some granitoids are intruded into the North China Platform (Nozawa and others, 1988). During the Proterozoic, various sizes and types of intrusive rocks were distributed on the North China and Yangtze Platforms and as relatively small bodies on the Kontum Platform and as the Chukotskiy Peninsula.

Early Paleozoic intrusive rocks are generally restricted to continental margins and paleomobile belts, such as the Siberia-Mongolia, Kunlun-Qinling, and Qilian Fold Belts. In contrast to the early Paleozoic, late Paleozoic granitic intrusive rocks are more widely distributed, mainly along the marginal areas of Eurasia continent.

During the Triassic to Paleogene, vigorous felsic to intermediate magmatism accompanied by many granitic intrusions took place in and around the platforms, massifs, and mobile belts. The Neogene intrusive bodies, mainly granodiorite and monzogranite, are generally small and occur in island-arc regions such as Kamchatka, Japan, Taiwan, and the Philippines.

Contrasting granitoids are identified; the I-type and S-type rocks of Chappell and White (1974) and the magnetite-series and ilmenite-series granitoids of Ishihara (1977). The S-type granitoids are compositionally restricted to granite and are magnetite free. This type has higher $\delta^{18}O$ values and initial $^{87}Sr/^{86}Sr$ ratios compared with the I-type granitoids and seems to have been generated from the upper continental crust as a result of anatexis of carbon-bearing sedimentary rocks. On the other hand, I-type granitoids are not compositionally restricted and consist mainly of felsic to intermediate rocks. This type is composed of both magnetite series and ilmenite series and is characterized by lower $\delta^{18}O$ values. This type of granitoid has been derived from igneous source materials of continental crust (Chappell and White, 1992).

Many of the mineral deposits in the principal orogenic belts are obviously related to intrusive rocks. Magmatic segregation occurred and pegmatite-greisen, skarn, porphyry, and various hydrothermal-replacement vein deposits formed in and around the intrusive rocks. According to Ishihara (1981), almost all porphyry copper and molybdenum deposits are associated with the magnetite-series granitoids, while tin-tungsten deposits are formed in and around the ilmenite-series granitoids. Thus, oxygen fugacity of intrusive magmas is one of the most critical parameters to control kind of metal resources (Ishihara, 1984).

Some nickel-copper-cobalt and vanadiferous titanomagnetite deposits are mainly related to magmatic segregation or unmixing of mafic to ultramafic intrusive rocks. Almost all of the intrusive rocks accompanied by nickel sulfide mineralization are intruded along deep fractures, mainly at the margins of Precambrian cratons and in Caledonian fold belts (Tang and Ren, 1987). In the western part of the Yangtze Platform, many of the nickel-copper-cobalt and vanadiferous titanomagnetite deposits that formed during the late Caledonian (early Paleozoic) to early Hercynian orogenic cycle are distributed along several north-trending deep fractures. They seem to have intruded after the segregation or unmixing of sulfide and oxide ores and rock-forming minerals in a magma chamber (Yao, 1988).

PEGMATITE, GREISEN, AND SKARN DEPOSITS

In and around other felsic intrusions, pegmatites and greisens occur, in which rare-earth metals such as niobium, tantalum, lithium, beryllium, tin, tungsten, and gemstones are concentrated. Industrial minerals such as quartz, feldspar, and mica from pegmatites are becoming increasingly important sources for ceramic and, recently, for electroceramic raw materials. Although these pegmatites and greisens are generally too small to show each body or zone at the map scale, small-scale mining is being carried out. In many cases, the concentrated areas of pegmatites and greisen zones are important sources for secondary-enrichment bodies of rare metals, especially rare earths, by weathering and alluvial processes.

Skarns are mainly composed of pyroxene, amphibole, garnet, and wollastonite formed by contact metamorphism between intermediate to felsic intrusive rocks and carbonate-dominant sedimentary rocks. Principal metallic elements of the skarn deposits–tin, tungsten, molybdenum, iron, copper, and lead-zinc–are precipitated after the skarn stage. Skarn deposits are one of the most important deposit types in this quadrant and are mainly distributed on the Siberian, North China, and Yangtze Platforms, and in the South China, Yunnan-Malayan, Sikhote-Alin, and Southwest Japan Fold Belts, where various intrusive rocks formed during four orogenic cycles: Caledonian, Hercynian, Early Alpine (Mesozoic), and Late Alpine (Cenozoic).

In the Angala-Ilim Province of the southern Siberian Platform, many skarn-type iron deposits (for example, Krasnoyarova and Korushnova) (table 1) are associated with gabbroic and diabasic Caledonian intrusive rocks (Sokolov and Grigor'ev, 1977). Although many granitic rocks were intruded into pre-Hercynian basement during the Hercynian orogenic cycle, no distinctive mineralization is recognizable, except some medium- to small-sized iron, copper, and tungsten deposits in China (Zhao and others, 1990) and iron-tin-bearing skarn deposits such as Bukit Besi and Pelapah Kanan (table 1) (Chu and others, 1988) in the eastern granite belt of the Malay Peninsula (Hutchison and Taylor, 1978).

Intense felsic magmatism occurred mainly in the Thai-Malay-Indonesia and south-to-east China-South Korea-Southwest Japan-Sikhote Alin belts during the Indosinian and Early to Late Alpine Orogenies. The granitoids in the Thai-Malay-Indonesia belts are accompanied by medium- to small-sized tin-tungsten-bearing deposits, typically in the Kinta Valley of Malaysia, where largely mined-out cassiterite-bearing skarn deposits (for example, Beatrice pipe) formed around the contact boundaries between Triassic S-type and ilmenite-series granitoids and Permo-Carboniferous carbonaceous sedimentary rocks.

The most intensive felsic magmatism occurs in the early to middle Yanshanian Orogeny (Jurassic) in China, the Bulgugsa Orogeny (Cretaceous) in South Korea, the Hiroshima disturbance (Late Cretaceous) in Japan, and the Sikhote-Alin orogenic belt in Russia. They are accompanied by skarn, porphyry copper-molybdenum, and hydrothermal mineralization during the Early Alpine Orogeny. Representative iron- and iron-copper-bearing skarn deposits are found in the Daye and Tonglian Mines (table 1) in China (Wang, 1986) and the Kamaishi Mine in Japan (table 1). Large-sized tungsten and tin deposits occur mainly in China (Dachang, Gejiu, Shizhuyuan, and Xianghualing) and in Korea (Sangdong) (Ishihara, 1984). Lead-zinc deposits include Shuikoushan, Huangshaping, and Xianghualing in China, Yeonhwa in Korea, and Kamioka and Nakatatsu in Japan. The Yangjiazhangzi deposit in China is representative of molybdenum-bearing skarn-type mineralization (table 1) (Liu, 1986b).

Comparatively small- to intermediate-sized felsic to intermediate stocks are mainly distributed in the Late Alpine orogenic belts in the island arcs of the western Pacific region: the outer belt of southwest Japan, the Philippines, Sumatra, Java, Irian Jaya, and Papua New Guinea. Some granitic intrusive rocks are associated with tin, copper, and zinc mineralization. Thanksgiving (table 1) copper-zinc, Philippines (Zanoria and others, 1984), Chichibu iron-copper-zinc (Ishihara, 1984) and Ho-ei tin-zinc, Japan, and Tembagapura (Ertsberg) copper-gold, Irian Jaya, Indonesia (table 1) (Titley, 1975) are outstanding deposits formed during the Late Alpine orogenic cycle.

PORPHYRY DEPOSITS

Porphyry copper and porphyry copper-molybdenum deposits in this quadrant formed from the Proterozoic to Cenozoic. Porphyry ores derive their name from the texture of granitic intrusive rocks in which phenocrysts of quartz and feldspar are enclosed by fine-grained groundmass of the same composition. In general, porphyry-type deposits have large reserves but are of low grade, with less than 1 percent copper. The main ore minerals are copper and iron sulfides, usually associated with gold, silver, and molybdenum. In some cases, molybdenum and rarely tungsten are the main ore minerals.

The geotectonic setting is intimately related to the intrusive rock type. Most island-arc intrusive rocks are quartz diorite and granodiorite in composition, whereas continental-margin intrusive rocks are quartz monzodiorite to quartz monzonite or granite (Kesler and others, 1975). Initial Sr ratios of the related intrusive rocks from island-arc regions are lower than 0.705, whereas those from cratonic continental margins exceed 0.705. Ishihara (1984) shows that porphyry copper deposits with small amounts of molybdenum and gold are representative of the magnetite-series granitic terranes, especially around the circum-Pacific orogenic belt. Differences between the two types of magma may reflect contamination from the crust when the mantle-derived magma ascended (Hutchison, 1983).

In general, porphyry copper deposits comparatively rich in gold were formed in island-arc terranes of Late Cretaceous to Quaternary age, and those rich in molybdenum occur at continental margins, regardless of geologic age. Representative porphyry copper-gold deposits of the western Pacific include Atlas, Dizon, and Sipalay (table 1) in the Philippines (Philippine Bureau of Mines and Geosciences, 1986), Tombulilato and north Sulawesi in Indonesia (Lowder and Dow, 1978), and Ok Tedi, Frieda, Wau, and Panguna in Papua New Guinea (table 1) (Metal Mining Agency of Japan, 1992).

In the porphyry copper deposits of the Philippine islands, the main accessory metal is gold (0.3 grams/ton) and accompanied with very small quantity of molybdenum (0.007 percent) (Hutchison, 1983). The deposits from Papua New Guinea and Indonesia (Cenozoic in age) also have a high gold content. Typical porphyry molybdenum deposits occur in the Qinling suture associated with high-silica granites of Late Mesozoic age (e.g. Nannihu and Jinduicheng) (table 1). The oldest porphyry copper deposits are Zhongtiaoshan (copper-molybdenum), formed during the Proterozoic (Liu, 1986a and b). They occur along the southern margin of the North China Platform. The Erdenet (copper-molybdenum) and Tsagaan-Suvrag (copper-molybdenum) deposits, Mongolia (Zhamsran and others, 1986), and Badaguan (copper-molybdenum) and Duobaoshan (copper-molybdenum) deposits, China, are related to granodioritic intrusive rocks of the Hercynian Orogeny (Rui and others, 1984) in the Siberia-Mongolia Fold Belt.

On the eastern part of the Yangtze Platform, many porphyry copper (the Dexing Mine), copper-molybdenum (Chengmenshan Mine), and copper-iron deposits (the Tongshankou Mine) (table 1) are closely associated with skarn mineralization of the early Yanshanian Orogeny (Mesozoic) (Liu, 1986a). Several porphyry copper-molybdenum deposits (Yulong and Melasongduo) related to monzonitic granites of the Late Alpine Orogeny occur in the Songpan-Garze Fold Belt (Rui and others, 1984).

VEIN DEPOSITS

Considerable amounts of gold-silver, copper, lead-zinc, tin, tungsten, molybdenum, antimony, mercury, and fluorspar are found in hydrothermal vein deposits. Although vein-type deposits are not as large as others, their ore grade is remarkably high in some areas, and the deposits are commonly exploited by small-scale underground mining. Recently, many epithermal gold-silver veins have been found in the western Pacific, especially in island-arc regions, due to active exploration during the 1980s in Kalimantan, Borneo, north Sulawesi, Papua New Guinea, the Solomon Islands, and Japan. The Hishikari epithermal gold-silver mine in Kagoshima, Japan, (table 1) is a typical example of high-grade (70 grams/ton of gold on average) medium-sized deposits formed during the Pleistocene (Izawa and others, 1990).

A large lead-zinc vein deposit being mined in south China (the Taolin Mine) (table 1) occurs in shear zones in Proterozoic sediment near Yanshanian granite intrusive rocks (136 Ma) located on the central part of the Yangtze Platform (Wang, 1987). A high-grade, indium-bearing, lead-zinc-silver polymetallic vein deposit at the Toyoha Mine (table 1) in Hokkaido, Japan, is one of the youngest mineral deposits associated with strong geothermal activity (Ohta, 1991).

Veinlets and vein swarms are the major source of detrital cassiterite placer deposits, especially in the Thai-Malaysia-Indonesia region. In south China, numerous tungsten deposits (for example, Xihuashan, Dangping, and Guimeishan) (table 1) are found mainly in and around the granitoids of the early Yanshanian Orogeny. Approximately half of the tungsten reserves and almost all of the tungsten ore in China comes from quartz veins (Liao, 1986).

TERRESTRIAL VOLCANIC ROCKS

Terrestrial volcanism has occurred principally in three geotectonic environments–intra-continental, continental-margin, and island-arc. Each is characterized by different igneous rock series. Almost all of the mobile belts since the Caledonian Orogeny have been covered by terrestrial volcanic rocks. The vast area extending from the South China Fold Belt to the Sikhote-Alin Fold Belt through the Gyeongsang Basin in South Korea and the Southwest Innerzone of Japan is an especially good example of intense terrestrial volcanism from the Late Jurassic to the Paleogene. Terrestrial volcanic activity took place on the continent, continental margins, and island arcs from the Neogene to the Quaternary. These volcanic rocks range from mafic (mainly basaltic) to felsic (rhyolitic); intermediate (andesitic) rocks are predominant in the island-arc regions–such as the Kuril Islands, Japan, the Philippines, Sumatra, Halmahera, Banda Arc, Papua New Guinea, and the Solomon Islands.

The mineral deposits related to volcanic activity are characterized by mercury, antimony, manganese, sulfur, lead-zinc, gold-silver, kaolin-pyrophyllite, and other industrial raw materials. Present-day geothermal and paleogeothermal systems related to intermediate to felsic volcanism have been the driving force in the formation of epithermal gold-silver, lead-zinc, and kaolin-pyrophyllite deposits. In the Philippines almost all of the epithermal gold-silver deposits (for example, Antamok, Acupan, and Mesbate) (table 1) are genetically related to late Miocene to Pleistocene andesitic volcanism (Mitchell and Balce, 1990). The central region of Kalimantan, Indonesia, is composed mainly of Tertiary volcanic, continental and marine sedimentary rocks, and several epithermal gold-silver deposits formed within a northeast-trending belt (Van Leewen and others, 1990). Many gold and copper-gold mineralized zones occurring as disseminated, stockwork, and lode-vein have been recently explored in northern Sulawesi, Indonesia. Along the Central Range of Papua New Guinea, there is considerable volcanogenic gold-silver mineralization together with porphyry copper mineralization (Ok Tedi, Frieda, and Wau) (table 1) closely related to the same late Miocene to Pliocene magmatism (Knight, 1975). In Lihir Island region, part of the Solomon Arc, the Lihir/Ladolam gold-silver deposit with large reserves was formed in the hydrothermal breccia zone of a Pleistocene caldera.

No significant antimony and mercury deposits occur in the island-arc regions, but many small- to medium-sized deposits are closely associated with terrestrial volcanic activity. Sulfur and pyrite deposits occur mainly in Pleistocene to Quaternary volcanic areas, such as Kamchatka, the Kuril Islands, Japan, Sumatra, and Banda Arc (Radkevich, 1979; Sudo and others, 1992; Djumhani, 1981).

Kaolin and pyrophyllite, major industrial raw materials, were formed mostly during two periods: Cretaceous to early Tertiary and late Tertiary to Quaternary. This important pyrophyllite-kaolin province was formed in the South China Fold Belt, the Gyeongsang Basin of South Korea, and the Southwest Innerzone of Japan.

SURFICIAL DEPOSITS INCLUDING PLACERS

Unconsolidated surficial mineral deposits–beach and alluvial placers, residuals, and brines and evaporites–are grouped under this category. The most common and widespread placer deposits consist of heavy and chemically stable minerals such as gold, chromite, cassiterite, magnetite, ilmenite, rutile, monazite, xenotime, zircon, and diamond.

The most important residual mineral resource of this quadrant is cassiterite, occurring in submerged beach and alluvial placers. Tin production from the Tin Belt–Thailand, Malaysia, and Indonesia–has supplied nearly half of the western world's demand, although production has been decreasing during the last decade (Carlin, 1992). The major tin sources are in braided streams, piedmont fans, and residual alluvial placers. The largest placer tin field, Kinta Valley, Malaysia, is located on late Paleozoic carbonate rocks and the Main Range granites of Triassic age (Hutchison, 1983). In the Kinta Valley, old alluvium (Stauffer, 1973) overlying basement rock contains a considerable amount of cassiterite and other heavy minerals, and is unconformably overlain by alluvium of Holocene age (Batchelor, 1979). Tantalum-bearing minerals–ilmenite, monazite, xenotime, and zircon–are found in this type of sediment. Some 50 percent of the world supply of tantalum comes from tin slag (Cunningham, 1991). The highest tantalum content is found in the tin slag of Thailand, probably derived from the western granite belt.

Considerable amounts of ilmenite and zircon are found as principal heavy minerals in beach placers in south China, southern Java, Indonesia, Malaysia, Thailand, Korea, and Japan. On the Malay Peninsula, mainly in Malaysia, monazite and xenotime, as well as ilmenite and zircon, are recovered from "amang", the heavy-mineral sand concentrate remaining after cassiterite is removed (Hedrick, 1992).

Sapphire and ruby occur mainly in Quaternary gravel beds distributed in central to eastern Thailand and west Kampuchea (Cambodia). The gemstones are derived from corundum-bearing basalt erupted during the Pleistocene on and around the Kontum Platform (fig.1) (Veeraburus and others, 1981).

Placer diamond deposits have been exploited so far by small-scale mining methods, except in the Siberian region. The northeastern margin of the Siberian Platform, the southeastern Liaodong Peninsula of the North China Platform, and the west and central areas of Kalimantan, Borneo, are placer diamond-producing areas. In southwest Kalimantan, almost all diamonds have been produced from Quaternary river terraces and gravel (Sigit and others, 1969).

Numerous placer-gold deposits of varying size occur in this quadrant. Comparatively large deposits are located at Stanovoy and northeast of Lake Baykal, on the southern margin of the Siberian Platform, and at the southern flank of the Kolyma Massif (Committee on Geology and Mineral Resources Utilization, Government of Russian Federation (CGMRUG), 1991).

SEAFLOOR RESOURCES

Seafloor deposits shown on the map include ferromanganese nodules, hydrothermal sulfide deposits, phosphorites, and heavy-mineral sand deposits. The information available on sulfide deposits, phosphorites, and heavy-mineral sands is so limited as to preclude estimating abundance; we have merely denoted their locations. Greatest attention has been devoted to the abundance and metal content of nodules.

Nodule abundance (seafloor coverage) at discrete locations has been ascertained from seafloor photographs and sediment cores. The nickel, copper, cobalt, and manganese contents of nodules in many of the core samples and in dredge samples have also been shown, rather than their iron content or other minor element composition. The aim of this section is to explain the procedures used to display these data.

Ferromanganese crust, recovered by dredging, is also shown on the map. No attempt is made to show all dredge sites. They are divided into four groups, based on their elemental contents (Lane and others, 1986; Manheim and Lane-Bostwick, 1989).

SEAFLOOR SEDIMENT

By
Floyd W. McCoy, University of Hawaii

Seafloor sediment is classified in four categories by its dominant component: (1) calcareous debris (calcareous ooze/clay or marl), (2) biosiliceous material (biosiliceous ooze/mud/clay), (3) terrigenous clastics (gravel/sand/silt), and (4) clays (including pelagic clay). These 4 sediment types are generalized from the 13-category classification scheme used to depict surficial deposits on the various circum-Pacific geologic quadrant maps, a scheme defining 30-60 percent boundaries for sediment nomenclature following that devised by Murray and Renard (1891). On the Northwest Quadrant Mineral-Resources Map, a stippled pattern is superimposed where coarse-grained particles (gravel, sand, or coarse-silt sizes) form greater than 15 percent of the sediment (for example, silty or sandy clay, volcanic gravel/sand/silt; calcareous gravel/sand/silt, or biosiliceous silt).

Sedimentary components were identified and abundances estimated via smear-slide analyses of core-top deposits in piston and gravity cores archived at the Lamont-Doherty Earth Observatory. Quantitative control came from analyses of $CaCO_3$ on selected samples. Additional smear-slide and $CaCO_3$ data came from published and unpublished sources. These data formed a primary data base for plotting sediment distributions. A secondary data base was constructed from general sediment descriptions in the literature that lacked quantitative component and $CaCO_3$ information; this information was used to estimate the geographic extent of distribution patterns. Information from Deep Sea Drilling Project (DSDP) samples were not incorporated because rotary drilling techniques do not recover undisturbed seafloor sediment. Data available at the time of map compilation from Ocean Drilling Program (ODP) sampling by hydraulic piston corers were incorporated. For clastic debris, the Wentworth grade scale was used. Constraints, problems, and assumptions in establishing these data bases and using them for mapping are discussed in greater detail in the various Explanatory Notes pamphlets that accompany each quadrant map of the Geologic Map series.

For simplification on the Northwest Quadrant Mineral-Resources Map, stations where surficial sediment was sampled or identification of sediment criteria derived from primary/secondary data bases are not shown; refer to the Northwest Geologic Map for this information (Inoue, 1988).

Mapping boundaries of sediment types were controlled by bathymetry, regional water depth of the calcite compensation depth, proximity to land (including knowledge of local geology), documented seafloor sedimentation processes, and the deposits left by this activity, as well as oceanographic/biologic phenomena.

This map depicts unconsolidated sediment recovered primarily by coring and presumably exposed on the ocean floor at the sediment/water interface. This sediment is not necessarily of Holocene age, nor is it necessarily the result of Holocene sedimentary processes.

FERROMANGANESE NODULES

By
David Z. Piper and Theresa R. Swint-Iki, U.S. Geological Survey

Nodules, consisting mainly of manganese and iron oxides, were first recovered from the Pacific Ocean by HMS *Challenger* during its voyage from 1872 to 1876 (Murray and Renard, 1891). They were most frequently recovered from abyssal depths where the bottom sediment is composed of red clay. Analyses of samples collected during that cruise, as well as of many samples collected subsequently, showed contents of nickel, copper, and cobalt in the range of a few tenths of one percent to about three percent. Interest in mining these deposits developed following a series of papers by Mero (1959, 1965) who called attention to the feasibility of their commercial recovery. McKelvey and others (1983) suggested that molybdenum, vanadium, and several of the rare earth elements might also be recoverable as by-products of possible future extractions of nickel, copper, and cobalt. These elements, as well as titanium, zinc, barium, lead, strontium, and yttrium, are present in the nodules in the range of ≤ 0.0l to nearly 0.1 percent (McKelvey and others, 1983).

Mero (1965) outlined the features of the geographic distribution of nodules in the Pacific Ocean and the regional variations in their composition. More recent studies include those by Cronan and Tooms (1969), Piper and Williamson (1977), and Calvert (1978), and still others are reported in the compendia of Glasby (1976), Bischoff and Piper (1979), and Sorem and Fewkes (1979). Other efforts to delineate the distribution of nodules on maps include those of Ewing and others (1971), Frazer and others (1972), Cronan (1977; 1980), Rawson and Ryan (1978), and McKelvey and others (1979, 1983).

These maps suggest that nodule occurrence and composition in the Pacific Ocean exhibit a rather uniform distribution over areas as great as several thousand square kilometers. Both parameters, however, show uneven variations on the scale of a few tens of square meters. For example, nodule coverage at individual stations, in the area of Hohnhaus Seamount at lat 14° N and long 179° W, ranges from 0 to greater than 50 percent. Furthermore, coverage at several of these stations ranges from 0 to 75 percent. Such variability (patchiness) makes it extremely difficult to estimate seafloor coverage on any scale, and particularly at the scale of this map. All maps showing the distribution of abundance and metal content at such scales have, therefore, a significant degree of uncertainty. Individual data points of nodule abundance and metal content are shown on the map by sets of symbols in order to permit evaluation of the procedures used in the contouring, which are explained below.

Ideally, nodule abundance should be expressed in mass per unit area; for example, kilograms per square meter. Such data, however, are sparse and the abundance is therefore shown in terms of percentage of the sea floor covered. No attempt is made to convert seafloor coverage to mass per unit area for three reasons. (1) Photographs may underestimate the seafloor coverage by as much as 25 percent, because nodules often are partially covered by a layer of "fluffy" sediment 5 to 15 mm thick (Felix, 1980). The degree to which they are covered is likely to vary between areas with different seafloor environments and with different nodule morphologies; it varies considerably even between box cores from a single relatively small area. (2) No simple relation exists between nodule cross-sectional area and nodule volume; nodule shapes vary from roughly spherical to strongly discoidal (Sorem and Fewkes, 1979). (3) Photographs are taken with the camera nearly on the bottom to as much as several meters above the bottom, thus making it impossible to ascertain nodule size accurately from the photographs.

Nodules are identified on the bottom photographs as dark and roughly equidimensional objects, with the entire population having a distribution strongly peaked in the size range of 1 to 12 cm in diameter. Angular objects and subrounded objects, often several tens of centimeters across, are identified as rock debris. In most cases, the difference between nodules and rocks is clear. Three people examined all photographs; still some errors in identification may have occurred.

Seafloor coverage of nodules was determined by comparing each photograph with templates showing a light background covered to varying degrees by black objects. The upper limit of 100 percent represents an arrangement of closest packing. The average coverage for all photographs at any one station was plotted as a single point. The number of photographs at most stations ranges from 1 to 850, although for most stations it is between 5 and 15.

Data from sediment cores (including box, gravity, and piston cores) supplement the photographic data. Core stations are plotted merely as recovering or not recovering nodules. Although the core sizes vary from a half meter on a side (box cores) to a 2.5-cm diameter (gravity cores), integrating these measurements with the photographic data was achieved in the following way.

Areas of varying seafloor coverage of nodules were delineated initially by using only the data obtained from the seafloor photography. In areas for which abundant cores were available, seafloor coverage was further refined using the core data. A contour of one percent was drawn to exclude areas in which photo stations recorded zero coverage. Several sediment cores recovered nodules in these areas, but the coverage outside this contour is certainly less than 1 percent and probably less than 0.1 percent. The position of the 1-percent contour was further defined by using the core data in two ways: (1) a nodule-bearing core was allowed in the <1-percent area only when its five nearest neighboring cores did not recover nodules, and (2) the contour was drawn to exclude all areas having at least 20 cores, of which 10 percent or fewer recovered nodules. In most areas as large as 12,000 km^2, cores recovering nodules average less than 1 percent of the total number of cores.

The second step was to draw the 50-percent contours to include both photographic stations of greater than 50 percent coverage and areas where recovery of nodules was greater than 75 percent.

The 10-percent contours were then drawn. This contour enclosed photographic stations that showed the complete range of coverage. Emphasis was placed, however, on photographic stations that showed greater than 25 percent coverage. Some photographic stations that recorded greater than 25 percent coverage lie outside the 10-percent contour line if their nearest neighbor recorded zero percent coverage or if 4 of 5 nearest cores failed to recover a nodule.

The 25-percent contours were drawn lastly to enclose areas of high coverage, as supported by either core or photographic data.

The percentage of cores recovering nodules between the 1-percent and 10-percent contours is surprisingly high: within all quadrant maps of the Pacific Ocean, nodule recovery varied from 8 to 70 percent and averaged 40 percent in areas containing more than 10 cores. In the areas where contours define nodule coverage at 10-25 percent, nodule recovery by cores averaged 55 percent and ranged from 25 to 62 percent. For the area of 25-50 percent coverage, nodule recovery by cores averaged 64 percent and ranged from 30 to 92 percent. In the area where coverage exceeded 50 percent, nodule recovery by cores averaged 83 percent. High nodule recovery rates, however, are less strongly suggested by the data from this quadrant. One possible explanation for high recoveries by cores in the other quadrants is that we have not distinguished between box cores, which sample a relatively large surface area of the sea floor, and gravity and piston cores. Alternatively, seafloor coverage based on bottom photographs may be biased on the low side owing to sediment cover.

Dredge hauls were not used as a supplement to the photographic and core data because the area sampled by dredging generally is not accurately known.

Nodules were divided according to their chemical composition into four partly overlapping categories: (1) greater than 1.8 percent nickel plus copper, (2) 1.0 to 1.79 percent nickel plus copper, (3) greater than 35 percent manganese, and (4) less than 1.0 percent nickel plus copper (McKelvey and others, 1983). These categories are shown on the map for stations for which data were available in the Scripps Sediment Data Bank. Only one contour, that of 1.8 percent nickel plus copper, in the Central Pacific Basin, is shown and it is based largely on the data collected and published by McKelvey and others (1979). The problem of contouring the chemical data is similar to that encountered in contouring the coverage data. Small-scale variability precluded exclusion of all conflicting data from the area enclosed by the contour.

A single area of greater than 50 percent seafloor coverage is delineated by the contour in the Central Pacific Basin. This large area corresponds to the area in which the nodules frequently contain more than 1.8 percent nickel plus copper.

Nodules and crusts with high cobalt content (these include dredge material) occur in areas of elevated relief, such as the seamounts and ridges. In many areas where cobalt-rich nodules are present, encrustations of the same composition can exceed 2 cm in thickness (Manheim and Halbach, 1982). Nodules with high manganese content (>35 percent Mn) tend to be restricted to hemipelagic sediment, for example, the eastern margin of the Pacific as shown on the Northeast Quadrant map. The few analyses of nodules from this environment of the Northwest Quadrant suggest a similar chemical trend.

The distribution of nodules is strongly related to sediment lithology, shown on the map as a background to the nodule distribution, and to sediment accumulation rates, not shown on this map but included on a 1:17,000,000-scale map of the Pacific Basin (Piper and others, 1985). The distribution of nodules shows a strong preference for siliceous sediment and pelagic clay. They tend not to occur on calcareous sediment. Nodules are apparently further restricted to areas exhibiting sediment accumulation rates of less than approximately 5 mm per thousand years (Piper and Swint, 1984; Piper and others, 1987).

Many factors influence the rather complex pattern of sea-bottom sediment lithology. These include the supply of material to the sea floor and the secondary processes in the deep ocean that alter or redistribute that supply. The supply is controlled largely by (1) proximity to a source of alumino-silicate material and (2) primary productivity in the photic zone of the ocean. The source of silicates (clay minerals as well as coarse debris) may be local (marine volcanic activity) or terrigenous (continents contribute material via both rivers and the atmosphere). Primary productivity, on the other hand, controls the "rain" of biogenic detritus to the sea floor. This fraction consists mostly of siliceous and calcareous tests of planktonic organisms, but contains lesser amounts of phosphatic material and organic matter from the soft parts of organisms.

Secondary processes include the dissolution of organic matter at depth in the ocean and the redistribution of sediment by deep-ocean currents. The occurrence of calcareous sediment and the depth of the seafloor show a strong relation, owing to the dissolution of $CaCO_3$ in the deep ocean. This relation can be seen at several locations along the equator (McCoy, 1988). Calcareous mud predominates to a depth of approximately 4000 m, where it gives way to pelagic clay or siliceous sediment. The exclusion of calcareous debris in the deeper sediment is controlled by the balance between the rate of supply of $CaCO_3$ to the seafloor and its rate of dissolution. The latter increases with water depth, owing to the increase in the solubility of $CaCO_3$ with decreasing water temperature and increasing pressure.

Many measurements of deep-ocean bottom currents have been made, but their usually weak intensity and the complex seafloor bathymetry have combined to thwart attempts to evaluate quantitatively their importance as a control on sediment accumulation rates and thus indirectly on nodule distribution, except for several rather careful studies of a few small areas (Lonsdale, 1981).

The origin of nodules is still uncertain after more than 100 years of research. Their distribution in the Pacific Ocean as shown on this map and the other quadrant maps of the Pacific, however, exhibits rather strong relations to the lithology of surface sediment and to seafloor bathymetry, relations which may help to elucidate the question of nodule genesis.

Bottom photographs used in this study are from the Bundesanstalt für Geowissenshaften und Rohstoffe, Committee for Coordination of Joint Prospecting for Mineral Resources in South Pacific Offshore Areas (CCOP), Geological Survey of Japan, Hawaii Institute of Geophysics, Institut Francais de Recherches pour l'Exploitation de la Mer, Lamont-Doherty Earth Observatory, Kennecott Exploration, Inc., National Oceanic and Atmospheric Administration, Scripps Institution of Oceanography, Smithsonian Institution, U.S. Navy Electronics Laboratory, and from published literature (Zenkevich, 1970; Andrews and Meylan, 1972; Greenslate and others, 1978). The chemical data on the nodules are from the Scripps Institution of Oceanography Sediment Data Bank.

FERROMANGANESE CRUST

By
Frank T. Manheim and Candice M. Lane-Bostwick, U.S. Geological Survey

The cobalt values indicated in the map represent data normalized to a hygroscopic moisture and substrate- (detrital matter) free basis. The algorithm to obtain these values is given by $Co^* = Co \times 51.23/(Fe+Mn)$, as determined in Manheim and Lane-Bostwick (1987). Samples designated as being of possible hydrothermal origin are identified by $Mn/Fe > 5$ and $Co < 0.2$ percent. Some classes of samples are excluded; the data of Barnes (1967) in the Scripps Institution Nodule Data Bank, samples lacking Mn and/or Fe data (which do not permit normalization), and samples having $Mn < 5$ percent. Multiple samples at one location have been averaged.

The geographical distribution of samples has been largely published in Lane and others (1986). Discussion of the significance of cobalt distributions and of the development of the U.S. Geological Survey Ferromanganese Crust Database is given in Manheim (1986) and Manheim and Lane-Bostwick (1987). The majority of the ferromanganese crust analyses are from two sources; the U.S. Geological Survey World Ocean Ferromanganese Crust Database and the Scripps Institution Nodule Data Bank. These and other sources are described in Manheim and Lane-Bostwick (1987).

POLYMETALLIC SULFIDES

By
Theresa R. Swint-Iki, U.S.Geological Survey

The initial discovery of warm-water springs rising from mounds of hydrothermal sediment at the Galapagos spreading center (Corliss, 1971; Weiss and others, 1977) and sulfide deposits forming at active high-temperature discharge sites at lat 21° N on the East Pacific Rise (Spiess and others, 1980) confirmed that hydrothermal circulation at seafloor-spreading axes leads to the precipitation of metal sulfides from hydrothermal fluids strongly enriched in sulfide and metals (Von Damm and others, 1985a, 1985b). Several types of deposits (metal oxides and sulfides) form directly or indirectly from this hydrothermal activity at divergent plate boundaries. Locations of seafloor hydrothermal mineral occurrences discovered through 1993 are from Rona and Scott (1993) and Hannington and others (1994).

The thermal balance in oceanic crust along spreading axes is considered to be dominated by hydrothermal circulation and advective cooling because conductive heat-flow measurements taken along ridge crests consistently show lower than expected values (Lister, 1972; Sleep and Wolery, 1978). Models of hydrothermal processes in oceanic crust developed by Lister (1977, 1982), Sleep and Wolery (1978), Edmond and others (1979), Fehn and Cathles (1979), Bischoff (1980), and Fehn and others (1983) are largely based on investigations of seafloor-spreading axes in the northeast quadrant of the Pacific. Since the initial observations of hydrothermal activity along the Galapagos spreading center and segments along the East Pacific Rise, polymetallic sulfides have been found in backarc basins where seafloor spreading occurs above subduction zones along convergent plate boundaries. The occurrence of metal-enriched sediment (Fe, Mn, Cu, Zn, As, Ag, and Au) is also indicative of hydrothermal activity in regions of backarc basins (Cronan, 1989). West of Papua New Guinea, in a spreading zone of the western Woodlark Basin, an active hydrothermal field was recently discovered within the caldera of Franklin Seamount at approximately lat 10°S., long 152°E., during a 1990 cruise of R/V *Akademik Mstislav Keldysh* to explore for hydrothermal mineralization in the region (Lisitsyn and others, 1991).

Metalliferous sediments occur in the Manus Basin, a backarc basin northeast of Papua New Guinea (Von Stackelberg and Von Rad, 1990; Hannington and others, 1991). The Manus Basin, Mariana Trough, and Okinawa Trough regions have been examined to study hydrothermal processes in backarc basins; locations and bibliography of sites of seafloor hydrothermal mineral occurrences for the entire Pacific basin are listed in Rona and Scott (1993).

Inside the rift zone of the Manus Basin hydrothermal chimneys were observed at lat 3°09.7′S., long150°16.8′E., at a depth of 2500 m (Both and others, 1986). During a later investigation in 1990 by the R/V *Akademik Mstislav Keldysh*, five hydrothermal fields, three active and two extinct, were also discovered (Lisitsyn and others, 1993). Dredging in the region has recovered manganese-rich crusts of hydrothermal origin, indicating that this region may contain reserves of polymetallic sulfide deposits (Bolton and others, 1988).

Four locations within the Mariana Trough are shown on the map where hydrothermal minerals occur. At lat 14°N., long 145°E., fumarolic activity was reported at Esmeralda Bank, along the flanks of the submarine volcano in the Mariana Trough (Stüben and others, 1992). Further north, hydrothermal vents have been reported at lat 18°13′N., long 144°42.6′E., within the axial region of the Mariana Trough (Botz and Stoffers, 1992); active chimneys have been located at lat 13°24′N., long 144°04′E., (Johnson and others, 1993), hydrothermal mounds at lat 14°58′N., long 145°15′E., and disseminated sulfides at Deep Sea Drilling Project (DSDP) site 456 at lat 17°56.7′N., long 145°10.8′E. (Natland and Hekinian 1982).

Three sites are shown on the map in the region of the Okinawa Trough: hydrothermal mounds at lat 27° 34.4′N., long 127°08.6′E., and lat 27°15′N., long 127°04.5′E. (Halbach and others, 1989), and active hydrothermal fields with sulfide-sulfate chimneys at lat 28°23.5′N., long 127°38.5′E.

The northernmost deposit shown on the map is located at lat 55°25′N., long 167°16.3′E., in a forearc area near the Kamchatka pensinsula (Kamchatsky Polu Ostrok) at Piyp submarine volcano where chimneys were reported.

Much further work is required to evaluate the extent and composition of known seafloor polymetallic sulfide deposits along spreading centers at divergent plate boundaries, in backarc basins, and along island arcs to evaluate possible future economic potential of polymetallic sulfide deposits and to explore for new deposits.

PHOSPHORITES AND PHOSPHATIZED ROCKS

By

David Z. Piper and Theresa R. Swint-Iki, U.S. Geological Survey

Submarine phosphate deposits consist of rock encrustations, nodules, and pellets. They occur on the continental shelves of the western Pacific Ocean, on seamounts throughout the central region of the Pacific Basin (for example, the Musicians Seamount group), and on ridges and seamounts of the continental margin. Deposits of guano altered to apatite are located on many Pacific Ocean islands along the equator in this quadrant. They represented a major resource in the early part of this century. Of particular importance were the deposits on Nauru and Ocean islands. They are still being mined on Nauru (Piper and others, 1991).

HEAVY-MINERAL DEPOSITS

By
Gretchen Luepke, U.S. Geological Survey

Submerged beaches and river channels are favorable sites in the marine environment for the occurrence of concentrations of heavy minerals (placers) such as gold, platinum, chromite, rutile (TiO_2) and ilmenite ($FeTiO_3$). Beginning with the formation of the great ice sheets during the Quaternary, sea level has repeatedly fallen and risen more than 200 meters. As a result of sea-level fluctuation, fossil beaches are found both above and below present sea level. During this period, heavy minerals in placers are either disseminated seaward or follow the landward-moving surf zone (Cronan, 1992). Placer deposits on modern beaches are also shown because they are clues to the presence offshore of additional deposits.

Heavy-mineral deposits have been exploited in the Far East for years. Placer gold derived from erosion of epithermal and porphyry gold deposits in the western Pacific and Southeast Asia may have an especially great untapped resource potential, particularly in the East China Sea (Clark and Li, 1991a; Cronan, 1992). Nearshore and offshore marine placers occur within the coastal areas of south China, eastern Vietnam, northern Borneo, and the Philippines (Clark and Li, 1993).

Offshore cassiterite (tin) placers, particularly in the so-called Indonesian Tin Islands between Sumatra and Borneo, are associated with the Southeast Asian tin belt, which runs from Thailand and Malaysia to the north (Burns, 1979). In Tongah Harbor on Phujet Island, Thailand, tantalum is recovered from tin slags as a byproduct of offshore tin operations (Burns, 1979).

Vietnam has onshore placers containing ilmenite, zircon, monazite, and rutile and has great potential in its offshore areas. These placers, with such minerals as titaniferous magnetite, chromite, gold, zircon, rutile, monazite, and tin, are extensively exploited in the South China Sea (Clark and Li, 1993).

In the Philippines, a placer of chromite (44.3 percent Cr_2O_3 grade), allanite, and monazite occurs on Palawan, and deposits of ilmenite (24-55 percent TiO_2), zircon, and monazite occur on Luzon (Clark and Li, 1993). One of the longest and most successful offshore mining operations produced over 500,000 oz of gold by 1992 at Paracale Bay (Cronan, 1992). In Lingayen Gulf on the northwest coast of Luzon, titanomagnetite was recovered during the 1970s in water 3-10 m in depth; reserves in 1972 were estimated at around 7 million tons (Burns, 1979).

The Liaodong (North Korea) and Shangdong (China) peninsulas, rich in epithermal gold deposits, are sources for placer gold; these sandy coasts are the best provenance for placer gold deposits (Clark and Li, 1991b). Submarine morphological features—sand bars, shoals, sea-floor platforms, and submerged rivers within the Bo Hai Sea are also indications of placer gold. Littoral mineral placers in the Bo Hai area include gold (up to 5.2 g/m^3), zircon (>1 percent), titaniferous magnetite (20-30 percent concentrate), and a garnet (20 percent grade) beach placer on South Zhon Island, China (Clark and Li, 1991b). On China's Hainan Island, a placer deposit of ilmenite, zircon, and monazite with 52 percent grade ilmenite occurs. Ilmenite/zircon placers occur at Guangxi, Behia, and Guangdong, China (56 percent ZrO_2) (Clark and Li, 1993). Exploration for diamonds has taken place off the China coast (Cronan, 1992).

Taiwan has placer deposits of magnetite, ilmenite, zircon, and monazite; these deposits at one time contained placer gold and were mined by the Japanese during World War II (Chou, 1967). Titaniferous magnetite sand with associated monazites are concentrated in the northern beaches. Black monazite sands associated with ilmenite, rutile, and zircon occur along the beaches and streams in western Taiwan; reserves are estimated at 500,000 tons, with grades ranging from 3 to 7 percent TiO_2 (Clark and Li, 1991a).

Titaniferous magnetite deposits occur in many coastal areas of Japan and the northern Philippines (Clark and Li, 1991a). In Japan, at Ariake and Kagoshima Bays in the southern part of Kyushu Island several million tons of ironsands (magnetite and ilmenite) were removed during the 1960s. At Ariake Bay, a 4-m thick deposit occurred at a depth of 50 m, 600 m offshore, and contained 3-5 percent titanomagnetite. At Kagoshima Bay, the deposits occurred at depths of 15 to 20 m. Offshore mining of magnetite and garnet sands in Japan has now ceased (Cronan, 1992).

In Russia, small placer gold deposits, part of the Zolotny Ridge gold-bearing district, are known along the shoreline of Anadyr Bay in modern marine sedimentary rocks (Gorodinsky, 1993). Deposits of gold occur near Kamchatka, and exploration for gold is ongoing off the Siberian coast (Cronan, 1992).

REFERENCES AND ADDITIONAL SOURCES OF DATA

Andrews, J.E., and Meylan, M.A., 1972, Results of bottom photography; *Kana Keoki* Cruise Manganese '72, *in* Investigations of ferromanganese deposits from the central Pacific: University of Hawaii Institute of Geophysics Report HIG-72-73, p. 83-111.

Asnachinda, P., and Pitragool, S., 1978, Review of nonmetallic mineral deposits of Thailand: Regional Conference on Geology and Mineral Resources of Southeast Asia, 3rd, Bangkok, 1978: Proceedings, p. 795-804.

Bai, G., and Yuan, Z., 1985, Carbonatite and related mineral resources: Beijing, Geologic Publication Company, Bulletin of Mineral Deposit 13, 192 p. [In Chinese with English abstract.]

Barnes,S.S.,1967,Minor element composition of ferromanganese nodules: Science, v. 157, p. 63-65.

Batchelor, B.C., 1979, Geological characteristics of certain coastal and offshore placers as essential guides for tin exploration in Sundaland, Southeast Asia: Geological Society of Malaysia Bulletin, v. 11, p. 283-313.

Bischoff, J.L., 1980, Geothermal system at 21°N, East Pacific Rise: physical limits on geothermal fluid and role of adiabatic expansion: Science, v. 207, p. 1465-1469.

Bischoff, J.L., and Piper, D.Z., 1979, Marine geology and oceanography of the Pacific manganese nodule province: New York, Plenum Press, 842 p.

Bolton, B.R., and others, 1988, Geochemistry and mineralogy of seafloor hydrothermal and hydrogenetic Mn oxide deposits from the Manus Basin and Bismarck Archipelago region of the southwest Pacific Ocean: Geology, v. 95, p. 65-87.

Borchert, H., and Muir, R. O., 1964, Salt deposits–the origin, metamorphism and deformation of evaporite: London, D. Van Nostrand Co., Ltd., 338 p.

Both, R., and others, 1986, Hydrothermal chimneys and associated fauna in the Manus Back-Arc Basin, Papua New Guinea: EOS, v. 67, May 27, 1986, p.489-490.

Botz, R.W., and Stoffers, P., 1992, Isotopic composition of hydrothermal precipitates from the Mariana Trough: Marine Geology, v. 108, p. 239-243.

Burns, V.M., 1979, Marine placer minerals, *in* Burns, R.G., ed., Marine minerals: Mineralogical Society of America Reviews of Mineralogy (Short Course Notes), v. 6, p. 347-380.

Calvert, S.E., 1978, Geochemistry of oceanic ferromanganese deposits: Philosophical Transactions of the Royal Society of London, v. 290A, p. 43-73.

Carlin, J.F., Jr., 1992, Annual report, Tin 1990: U.S. Bureau of Mines, 36p.

Chancharoonpong, K., 1978, Antimony deposits of Thailand: Special issue for 3d Conference of Geology and Resources of Southeast Asia, Journal of the Geological Society of Thailand, v. 3, p. E3—1-11.

Chappell, B.W., and White, A.J.R., 1974, Two contrasting granite types: Pacific Geology, no. 8, p. 173-174.

Chappell, B.W., and White, A.J.R., 1992, I- and S- type granites in the Lachlan Fold Belt: Royal Soc. Edinburgh, Earth Sci., v. 83, p. 1-26.

Chou, J.T., 1967, Heavy minerals in Taiwan: Taipei, Chinese Petroleum Corporation, 44 p.

Chu, L.H., Chand, F., and Singh, D.S., 1988, Primary tin mineralization in Malaysia; Aspects of geological setting and exploration strategy *in* Hutchison, C.S., ed., Geology and tin deposits in Asia and the Pacific: Berlin, Springer-Verlag, p. 593-613.

Chun, Q.S., and others, 1986, Early crusts and mineral deposits of Liaodong peninsula, China: Beijing, Geologic Publication Company, 575 p. [In Chinese with English abstract.]

Clark, A.L., and Li, C., 1991a, Marine mineral resources of the East China Sea—scientific and economic opportunities: Marine Mining, v. 10, no. 2, p. 117-144.

Clark, A.L., and Li, C., 1991b, Gold placer deposits in the Bo Hai Sea: Marine Mining, v. 10, no. 3, p. 195- 214.

Clark, A.L., and Li, C., 1993, Marine mineral resources of the South China Sea: Marine Georesources and Geotechnology, v. 11, no. 1, p. 101-126.

Commission for the Geological Map of the World (CGMW), Ray, D.K., ed., 1984, Tectonic map of south and east Asia: Paris, scale 1:5,000,000, with explanatory text.

Committee for Coordination of Joint Prospecting for Mineral Resources in Asian Offshore Areas (CCOP), 1981, Studies in east Asian tectonics and resources: Bangkok, CCOP, 250 p.

Committee on Geology and Mineral Resources Utilization, Government of Russian Federation (CGMRUG), 1991, Ilyin, K.B., Poluektov, V.N., Terentiev, V.M., and Shcheglov, A.D., eds., Map of mineral resources of Russia and adjacent countries: 4 sheets, scale 1:5,000,000.

Corliss, J.B., 1971, The origin of metal-bearing submarine hydrothermal solutions: Journal of Geophysical Research, v. 76, p. 8128-8138.

Corvalán, José D., Guild, P.W., Piper, D.Z., Swint-Iki, T.R., McCoy, F.W., and others, 1996, Mineral-resources map of the circum-Pacific region, southeast quadrant: U.S. Geological Survey, Circum-Pacific Map Series CP-44, scale 1:10,000,000, 30 p.

Cronan, D.S., 1977, Deep-sea nodules: distribution and geochemistry, *in* Glasby, G.P., ed., Marine manganese deposits: Amsterdam, Elsevier Publishing Company, p. 11-44.

Cronan, D.S., 1980, Underwater minerals: London, Academy Press, 362 p.

Cronan, D.S., 1989, Hydrothermal metalliferous sediments in the southwest Pacific, *in* Ayala-Castañares, A., and others, eds., Oceanography 1988: Universidad Nacional Autonoma de Mexico Press, Mexico D.F., p. 149-166.

Cronan, D.S., 1992, Marine minerals in exclusive economic zones: London, Chapman&Hall, 209p.

Cronan, D.S., and Tooms, J.S., 1969, The geochemistry of manganese nodules and associated pelagic deposits from the Pacific and Indian Oceans: Deep-Sea Research, v. 16, p. 335-349.

Cunningham, L.D., 1991, Annual report, Columbium (niobium) and tantalum 1990: U.S. Bureau of Mines, 19 p.

Diehl, P. and Kern, H., 1981, Geology, mineralogy. and geochemistry of some carbonate-hosted lead-zinc deposits in Kanchanaburi Province, west Thailand: Economic Geology, v. 76, p. 2128-2146.

Division of Regional Geology and Mineral Resources, eds., 1985, Monograph of manganese deposits in China: Beijing, Ministry of Geology and Mineral Resources, Geological Publishing House, 386 p. (in Chinese).

Djumhani, 1981, Metallic mineral deposits of Indonesia: A metallogenic approach, *in* Ishihara, S., and Sasaki, A., eds, Metallogeny of Asia: Geological Survey of Japan, Report no. 261, p. 107-124.

Drew, L.J., Meng, Q., and Sun, W., 1990, The Bayan Obo iron-rare-earth-niobium deposits, Inner Mongolia, China: Lithos, v. 26, p. 43-65.

Drummond, K.J., 1985, Mineral-resources map of the circum-Pacific region, northeast quadrant: Tulsa, Okla., American Association of Petroleum Geologists, scale 1:10,000,000, 48 p.

Duan, R., and Lu, Y., 1984, The temporal distribution of gold deposits in China: Bulletin of the Shenyang Institute of Geology and Mineral Resources, Chinese Academy of Geological Science, no. 9, p. 1-9.

Edmond, J.M., and others, 1979, On the formation of metal-rich deposits at ridge crests: Earth and Planetary Science Letters, v. 46, p. 19-30.

Ewing, M., Horn, D., Sullivan, L., Aiken, T., and Thorndike, E., 1971, Photographing manganese nodules on the ocean floor: Oceanology International, v. 6, no. 12, p. 26-32.

Fehn, U., and Cathles, L.M., 1979, Hydrothermal convection at slow spreading mid-ocean ridges: Tectonophysics, v. 55, no. 12, p. 239-260.

Fehn, U., and others, 1983, Numerical models for the hydrothermal field at the Galapagos Spreading Center: Journal of Geophysical Research, v. 88, p. 1033-1048.

Felix, D., 1980, Some problems in making nodule abundance estimates from sea floor photographs: Marine Mining, v. 2, p. 293-302.

Field, C.W., Wetherell, D.G., and Dasch, E.J., 1981, Economic appraisal of Nazca plate metalliferous sediments, *in* Kulm, L.D., and others, eds., Nazca plate–crustal formation and Andean convergence: Geological Society of America Memoir 154, p. 315-320.

Frazer, J.Z., and Fisk, M.B., 1980, Availability of copper, nickel, cobalt, and manganese from ocean ferromanganese nodules (III): Scripps Institution of Oceanography Report SIO 80-16, 31 August 1980, 117 p.

Frazer, J.Z., Hawkins, D.L., and Arrhenius, G., 1972, Surface sediments and topography of the north Pacific: Scripps Institute of Oceanography, Geologic Data Center, scale 1:3,630,000.

Glasby,G.P.,ed.,1976,Marine manganese deposits: Amsterdam, Elsevier Publishing Company, 523 p.

Golightly, J.P., 1981, Nickeliferous laterite deposits: Economic Geology, 75th Anniversary vol., p. 1905-1980.

Goossens, P.J., 1978, The metallogenic provinces of Burma; their definitions and geological extension into China, India, and Thailand: Regional Conference on Geology and Mineral Resources of Southeast Asia, Third, Bangkok, 1978: Proceedings, p. 431-492.

Gorodinsky, M.E., 1993, Significant placer districts of the Russian Northeast: Table 4, *in* Nokleberg, W., Jr., Bundtzen, T.K., Grybeck, Donald, Koch, R.D., Eremin, R.A., Rozenblum, I.S., Sidorov, A.A., Byalobzhesky S.G., Sosunov, G.M., Shpikerman, V.I., and Gorodinsky, M.E., eds., Metallogenesis of mainland Alaska and the Russian northeast: U.S. Geological Survey Open-File Report 93-339, p. 178-188.

Greenslate, J., Krutein, M., and Pasho, D., 1978, Initial report of the 1972 Sea Scope Expedition: Spokane, Wash., U.S. Bureau of Mines (Minerals Availability System), 3 vols.

Guild, P.W., 1981, Preliminary metallogenic map of North America; a numerical listing of deposits: U.S. Geological Survey Circular, 858-A, 93 p.

Guild, P.W., Piper, D.Z. and others, 1998, Mineral-resources map of the circum-Pacific region, Antarctic sheet: U.S. Geological Survey Circum-Pacific Map Series, Map CP-47, scale 1:10,000,000, 19p.

Guo, W., Liu, M., Wang, Y., Liu, L., Xu, G., Zhang, J., and Ku, J., 1987, The metallogenic map of endogenic ore deposits of China: Beijing, Cartographic Publishing House, scale 1:4,000,000, with explanatory text, 72 p. [In Chinese.]

Halbach, P., and others, 1989, Probable modern analoque of Kuroko -type massive sulfide deposits in the Okinawa trough back-arc basin: Nature, v. 338, p. 496-499.

Hannington, M.D., Herzig, P.M and Scott, S.D., 1991, Auriferous hydrothermal precipitates on the modern seaflooor *in* Foster, R.P., ed, Gold metallogeny and exploration: Glasgow and London, Blackie and Son Ltd., p. 250-282.

He, S., 1985, Geology and manganese mineralization in Zunyi area, Guizhou Province, Div. Regional Geology and Mineral Resources, Ministry of Geology and Mineral Resources, China, ed., Monograph of manganese deposits in China: Geol. Publ. House, Beijing, p. 106-119 [In Chinese.]

He, Yuejiao, and Zhu, Luxi, 1986, Mineral resources of China: Shanghai, Education Publishing House, 227 p. (in Chinese).

Hedrich, J.B., 1992, Annual report, Rare earths 1990: U.S. Bureau of Mines, 34 p.

Hutchison, C.S., 1983, Economic deposits and their tectonic setting: London, Macmillan Press, 365 p.

Hutchison, C.S., and Taylor, D., 1978, Metallogenesis in southeast Asia: Journal of the Geological Society of London, v. 135, p. 407-428.

Inoue, E., chair, 1987, Plate-tectonic map of the circum-Pacific region, northwest quadrant (revised from Nishiwaki, C., 1981): Houston, Circum-Pacific Council for Energy and Mineral Resources, scale 1:10,000,000, 14 p.

Inoue, E., chair, 1988, Geologic map of the circum-Pacific region, northwest quadrant: Houston, Circum-Pacific Council for Energy and Mineral Resources, scale 1:10,000,000, 30 p.

Ishihara, S., 1977, The magnetite-series and ilmenite-series granitic rocks: Mining and Geology of Japan, v. 27, p. 293-305.

Ishihara, S., 1984, Granitoid series and Mo/W-Sn mineralization in East Asia, *in* Shimazaki, Y., ed., Geologic evolution, resources, and geologic hazards: Geological Survey of Japan, Report no. 263, p. 173-208.

Izawa, E., Urashima, Y., Ibaraki, K., Suzuki, R., Yokoyama, T., Kawasaki, K., Koga, A., and Taguchi, S., 1990, The Hishikari gold deposit; high-grade epithermal veins in Quaternary volcanics of southern Kyushu: Journal of Geochemical Exploration, v. 36, p. 1-56.

Jia, E., 1986, Geological characteristics of the Jinchuan Cu-Ni sulfide deposit in Gansu Province: Mineral deposits, China:Beijing, Geological Publishing House, v. 5, p. 35-38. [In Chinese with English abstract.]

Johnson, H.R., and others, 1993, Hydrothermal vent deposits and two magma sources for volcanoes near 13°20'N in the Mariana back arc: a view from SHINKAI 6500: EOS, American Geophysical Union Transactions, v. 74, p. 681.

Kamitani, M., 1987, Bauxite deposits in China, on high-aluminous shale: Journal of Clay Science, Japan, v. 27, p. 62-71. [In Japanese with English abstract.]

Kanehira, K., 1970, Bedded cupriferous iron sulfide deposits in Japan, a review, *in* T. Tatsumi, ed., Volcanism and ore genesis: Tokyo, University of Tokyo Press, p. 51-76.

Kesler, S.E., Jones, L.M., and Walker, R.L., 1975, Intrusive rocks associated with porphyry copper mineralizations in island arc areas: Economic Geology, v. 70, p. 515-526.

Kim, S.E., and Hwang, D.H., 1983, Metallogenic map of Korea : Korea Institute of Energy and Resources, scale 1:1,000,000, with explanatory text 52 p.

Knight, C.L., 1975, Geology of Papua New Guinea, *in* Knight, C.L., ed., Economic geology of Australia and Papua New Guinea–l, Metals: Economic Geology, Monograph 5, p. 823-833.

Lane, C.M., Manheim, F.T., Hathaway, J.C., and Ling, T.H., 1986, Station map of the world ocean ferromanganese crust database: U.S. Geological Survey, Miscellaneous Field Studies Map MF-1869, 2 sheets and pamphlet, scales 1:30,000,000 and 1:5,000,000.

Li, C.Y., Wang, Q., Liu, X., and Tang, Y., 1982, Tectonic map of Asia: Beijing, Cartographic Publishing House, with explanatory note, scale 1:8,000,000.

Li, Y., 1986, Proterozoic and Cambrian phosphorites-regional reviews: China, *in* Cook, P.J., and Shergold, J.H., eds., Phosphate deposits of the world–Proterozoic and Cambrian phosphorites: London, Cambridge University Press, v. 1, p. 43-62.

Liao, J., 1986, Tungsten ore in China; the general situation of development and the classification of commercial deposits: Geology and Prospection, v. 21, no. 9, p. 11-16. [In Chinese.]

Lisitsyn, A.P., and others, 1991, Active hydrothermal activity at Franklin Seamount, western Woodlark Sea (Papua New Guinea): International Geology Review, v. 33, p. 914-929.

Lisitsyn, A.P. and others, 1993, A hydrothermal field in the rift zone of the Manus Basin, Bismarck Sea: International Geology Review, v. 35, no. 2, p. 105-126.

Lister, C.R.B., 1972, On the thermal balance of a mid-ocean ridge: Royal Astronomical Society Geophysical Journal, v. 26, p. 515-535.

Lister, C.R.B., 1977, Qualitative models of spreading-center processes, including hydrothermal penetration: Tectonophysics, v. 37, p.203-218.

Lister, C.R.B., 1982, "Active" and "passive" hydrothermal systems in the oceanic crust: predicted physical conditions, in K.A. Fanning and F.T. Manheim, eds., The dynamic environment of the ocean floor: Lexington, Mass., Lexington Books, p. 441-470.

Liu, C., 1988, The genetic types of bauxite deposits in China: Scientia Sinica, series B, v. 21, p. 1010-1024.

Liu, Jiayuan, and Shen, Jili, 1982, Metallogenic-magmatic systems of tungsten in Jiangxi Province, *in* Hepworth, J.V., ed., Symposium on tungsten geology, Kiangsi, China, 1981: Bandung, Indonesia, Economic and Social Commission for Asia and the Pacific/Regional Mineral Resources Development Center, p. 313-326.

Liu, L., 1986a, The geological setting of metallogenesis of main types of endogenic copper deposits in China and their regional distribution regularity, *in* Principal base metal deposits and their metallogeny in China: Chinese Environmental Sci. Publ. Co., p. 109-130. [In Chinese with English abstract.]

Liu, L., 1986b, The distribution regularity of endogenic Mo deposits in China and their metallogenic characteristics in China: *in* Principal base metal deposits and their metallogeny in China: Chinese Environmental Sci. Publ. Co., p. 44-64. [In Chinese with English abstract].

Liu, W., 1984, Regional tectonic setting of the stratabound lead-zinc deposits in carbonate rocks of east China: Bulletin of Mineral Deposits, 3, p. 38-46. [In Chinese with English abstract.]

Lonsdale, P., 1981, Drifts and ponds of reworked pelagic sediment in part of the southwest Pacific: Marine Geology, v. 43, p. 153.

Lowder, G.G., and Dow, J.A.S., 1978, Geology and exploration of porphyry copper deposits in north Sulawesi, Indonesia: Economic Geology, v. 73, p. 628-644.

Manheim, F.T., 1986, Marine cobalt resources: Science, v. 232, 2 May 1986, p. 600-608.

Manheim, F.T., and Halbach, P., 1982, Economic significance of ferromanganese crusts on seamounts of the mid-Pacific area: Geological Society of America, Abstracts with Programs, v. 14, p. 555.

Manheim, F.T., and Lane-Bostwick, C.M., 1987, World ocean ferromanganese crust database: Final Report to Minerals Management Service.

Manheim, F.T., and Lane-Bostwick, C.M., 1989, Chemical composition of ferromanganese crusts in the world ocean: a review and comprehensive database: U.S. Geological Survey Open-File Report 89-020, 450 p.

McCoy, F.W., 1988, Seafloor sediment, *in* Inoue, E., chair, Geologic map of the circum-Pacific region, northwest quadrant: Houston, Circum-Pacific Council for Energy and Mineral Resources, scale 1:10,000,000, 30 p.

McKelvey, V.E., Wright, N.A., and Rowland, R.W., 1979, Manganese nodule resources in the northeastern equatorial Pacific, *in* Bischoff, J.L., and Piper, D.Z., eds., Marine geology and oceanography of the Pacific manganese nodule province: New York, Plenum Press, p. 747-762.

McKelvey, V.E., and others, 1983, Analysis of the world distribution of metal-rich manganese nodules: U.S. Geological Survey Circular 886, 55p.

Mero, J.L., 1959, A preliminary report on the economics of mining and processing deep-sea manganese nodules: Berkeley, University of California Mineral Technology Institute of Marine Research, 96 p.

Mero, J.L., 1965, The mineral resources of the sea: Amsterdam, Elsevier Publishing Company, 312 p.

Metal Mining Agency of Japan (MMAJ), 1992, Geology and mineral resources of Southeast Asia and Oceania: Report of Committee for Geological Analysis, MMAJ, Tokyo, 456 p. [In Japanese.]

Mitchell, A.H.G., and Balce, G.R., 1990, Geological features of some epithermal gold systems, Philippines: Journal of Geochemical Exploration, v. 35, p. 241-296.

Mo, R., and others, 1989, Geology and graphite deposits in China: Beijing, Chinese Construction Industry Publ., 290 p. [In Chinese.]

Moore, G.W., 1986, Plate boundaries, *in* Inoue, E., chair, Plate-tectonic map of the circum-Pacific region, northwest quadrant: Tulsa, Okla., American Association of Petroleum Geologists, scale 1:10,000,000, 20 p.

Murray, J., and Renard, A.F., 1891, Report on deep-sea deposits based on the specimens collected during the voyage of H.M.S. *Challenger* in the years 1872 to 1876, *in* Thomson, C.W., and Murray, J., eds., Report on the scientific results of the voyage of H.M.S. *Challenger* during the years 1872-1876: New York, Johnson Reprint Corporation, p. 8-147.

Natland, J.H., and Hekinian, R., 1982, Hydrothermal alteration of basalts and sediments at Deep Sea Drilling Project site 456, Mariana trough: Deep Sea Drilling Project Initial Reports, v. 60, p. 759-768.

Nishiwaki, C., chair, 1981, Plate-tectonic map of the circum-Pacific region, northwest quadrant: Tulsa, Okla., American Association of Petroleum Geologists, scale 1:10,000,000, 14 p.

Nishiwaki, C., chair, 1985, Geodynamic map of the circum-Pacific region, northwest quadrant: Houston, Circum-Pacific Council for Energy and Mineral Resources, scale 1:10,000,000, 12 p.

Nishiwaki, C., and Uyeda, S., 1980, Tectonic control of porphyry copper genesis-stress regime at the time of ore emplacement: Mining and Metallurgical Institute of Japan (MMIJ)-American Institute of Mining, Metallurgical and Petroleum Engineers (AIME), Joint Meeting, Fourth, Tokyo,1980: Proceedings, 2 vols.

North American Metallogenic Map Committee, 1981, Preliminary metallogenic map of North America: U.S. Geological Survey, 4 sheets, scale 1:5,000.

Notholt, A.J.G., and Sheldon, R.P., 1986, Proterozoic and Cambrian phosphorites-regional review: world resources, *in* Cook, P.J., and Shergold, J.H., eds., Phosphate deposits of the world–Proterozoic and Cambrian phosphorites: London, Cambridge University Press, v. 1, p. 9-19.

Nozawa, T., Sato, T., Teraoka, Y., and Yoshida, T., 1988, Explanatory notes for the geologic map of the circum-Pacific region, northwest quadrant, *in* Inoue, E., chair, Geologic map of the circum-Pacific region, northwest quadrant: Houston, Circum-Pacific Council for Energy and Mineral Resources, scale 1:10,000,000, 30 p.

Ohta, E., 1991, Polymetallic mineralization at the Toyoha mine, Hokkaido, Japan: Mining Geology, v. 41, p. 279-295.

Palfreyman, W.D., chair, 1988, Geologic map of the circum-Pacific region, southwest quadrant: Houston, Circum-Pacific Council for Energy and Mineral Resources, scale 1:10,000,000, 37 p.

Palfreyman, W.D., and others, 1996, Mineral-resources map of the circum-Pacific region, southwest quadrant: U.S. Geological Survey Circum-Pacific Map Series, Map CP-42, scale 1:10,000,000, 40 p.

Park, N.Y., 1981, Geology and mineral deposits of Korea, *in* Ishihara, S., and Shimazaki, Y., eds., Metallogeny of Asia: Geological Survey of Japan, Report no. 261, p. 93-106.

Philippine Bureau of Mines and Geosciences, 1986, Geology and mineral resources of the Philippines: Manila, Bureau of Mines and Geosciences, Ministry of Natural Resources, v. 1, 446 p.

Piper, D.Z., Aharon, P., and Loebner, B.J., 1991, Physical and chemical properties of the phosphate deposit on Nauru, the equatorial Pacific, *in* Riggs, S., and Burnett, W., eds., Phosphate deposits of the world: London, Cambridge Press, v. 3, p. 178-194.

Piper, D.Z., and Swint, T.R., 1984, Distribution of ferromanganese nodules in the Pacific Ocean [abs.]: International Geological Congress, 27th, Moscow, 1984: Proceedings, v. 3, p. 64.

Piper, D.Z., Swint-Iki, T.R., and McCoy, F.W., 1987, Distribution of ferromanganese nodules in the Pacific Ocean: Chemica Erde, v. 46, p. 171-184.

Piper, D.Z., and Williamson, M.E., 1977, Composition of

Pacific Ocean ferromanganese nodules: Marine Geology, v. 23, p. 285-303.

Piper, D.Z., and others, 1985, Manganese nodules, seafloor sediment, and sedimentation rates map of the Circum-Pacific region, Pacific Basin: Tulsa, Okla., American Association of Petroleum Geologists, scale 1:17,000,000.

Radkevich, E.A., 1979, Metallogenic map of the Pacific ore belt: Vladivostok, Academy of Sciences of the USSR, Far East Geological Institute, 10 sheets, scale 1:10,000,000.

Rawson, M.C., and Ryan, W.B.F., 1978, Ocean floor sediment and polymetallic nodules: Palisades, New York, Lamont-Doherty Geological Observatory, Columbia University, scale 1:23,230,300.

Rona, P.A., and Scott, S.D., 1993, A special issue on seafloor hydrothermal mineralization: new perspectives: Economic Geology, v. 88, no. 8 (December 1993), p. 1933-1976.

Rui, Z., Huang, C., Qi, G., Xu, J., and Zhang, H., 1984, Porphyry copper(-molybdenum) deposits of China: Beijing, Geologic Publication Company, 350 p. [In Chinese with English abstract.]

Sato, T., 1981, Geology of Southeast Asia, a review, *in* Ishihara, S., and Sasaki, A., eds., Metallogeny of Asia: Geological Survey of Japan, Report no. 261, p. 7-19.

Schellmann, W., 1989, Composition and origin of laterite nickel ore at Tagaung Tagung, Burma: Minera Deposita, v. 24, p. 161-168.

Senathi, S., Lum, H.K., Lau, J.W.E., and Leong, K.M., 1975, Metallogenic map of Malaysia: Malaya Geological Survey Report, no. MX(G) 14, 37 p.

Shenyang Institute of Geology and Mineral Resources, 1986, Collected papers on geology of gold deposits in China: Beijing, Chinese Academy of Geological Sciences, Geological Publishing House, 356 p. (in Chinese).

Sigit, S., Purbo-Hadiwidjojo, M.M., Sulasumoro, B., and Wirjosudjono, S., 1969, Minerals and mining in Indonesia: Djakarta, Ministry of Mines, 123 p.

Sleep, N.H., and Wolery, T.J., 1978, Egress of hot water from mid-ocean ridge hydrothermal systems: some thermal constraints: Journal of Geophysical Research, v. 83, p. 5913-5922.

Sokolov, G.A., and Grigor'ev, V.M., 1977, Deposits of iron, *in* Smirnov, V.I., ed., Ore deposits of the USSR: London, Pitman Publishing, v. 1, p. 7-113.

Sorem, R.K., and Fewkes, R.H., 1979, Manganese nodules; research data and methods of investigation: New York, Plenum Press, 723 p.

Spiess, F. N., and others, 1980, East Pacific Rise: hot springs and geophysical experiments: Science, v. 207, p. 1421-1432.

Stauffer, P.H., 1973, Cenozoic, *in* Gobbett, D.J., and Hutchison, C.S., eds., Geology of the Malay Peninsula: west Malaysia and Singapore: New York, Wiley Interscience, p. 143-176.

Stüben, D., and others, 1992, First results of study of sulphur-rich hydrothermal activity from an island-arc environment: Esmeralda Bank in the Mariana Arc: Marine Geology, v. 103, p. 521-528.

Sudo, S., Yoshii, M., Kamitani, M., and Kouda, R., 1992, Mineral resources of Japan and adjoining areas, *in* Geological Atlas of Japan, 2nd edition: Geological Survey of Japan.

Sumii, T., and others, 1992, Energy-resources map of the circum-Pacific region, northwest quadrant: U.S. Geological Survey Circum-Pacific Map Series, Map CP-40, scale 1:10,000,000, 34 p.

Sun, H., 1983, A brief introduction of the mineral resources and production of less common minerals in China: Rare Metals, v. 2, p. 4-9.

Taira, A., and Tashiro, M.M., 1987, Late Paleozoic and Mesozoic accretion tectonics in Japan and Eastern Asia, *in* Taira, A., and Tashiro, M., eds., Historical biogeography and plate tectonic evolution of Japan and eastern Asia: Tokyo, Terra Scientific Publ. Co., p. 1-44.

Takenouchi, S., Shimazaki, H., Mariko, T., and Kamitani, M., 1987, Rare metals in China: Committee report of the Metal Mining Agency of Japan, 144 p. (in Japanese).

Tang, Z., and Ren, D., 1987, Types and metallogenic models of nickel sulphide deposits in China: Acta Geologia Sinica, China, no. 4, p. 350-361.

Titly, S.R., 1975, Geological characteristics and environment of some porphyry copper occurrences in the southwestern Pacific: Econ. Geol., v. 70, p. 499-514.

Tran, Q. and Nguyen, D.K., 1986, Proterozoic and Cambrian phosphorite-deposits; Lao Cai, Vietnam, *in* Cook, P.J., and Shergold, J.H., eds., Phosphate deposits of the world–Proterozoic and Cambrian phosphorites: London, Cambridge University Press, v. 1, p. 155-161.

United Nations Economic and Social Commission for Asia and the Pacific, 1985, Atlas of mineral resources of the Economic and Social Commission for Asia and the Pacific region—Malaysia: Economic and Social Commission for Asia and the Pacific, v. 1, scale 1:2,500,000 with explanatory text.

Van Leewen, T.M., Leach, T., Hawke, A.A., and Hawke, M.M., 1990, The Kelian disseminated gold deposit, East Kalimantan, Indonesia: Journal of Geochemical Exploration, v. 35, p. 1-16.

Veeraburus, M., Mantjit, N., and Suensilpong, S., 1981, Outline of geology and ore deposits of Thailand, *in* Ishihara, S., and Sasaki, A., eds., Metallogeny of Asia: Geological Survey of Japan, Report no. 261, p. 81-92.

Von Damm, K.L., Edmond, J.M., Grant, B., Measures, C.I., Walden, B. and Weiss, R.F., 1985a, Chemistry of submarine hydrothermal solutions at 21°N, East Pacific Rise: Geochimica et Cosmochimica Acta, v. 49, p. 2197-2220.

Von Damm, K.L., Edmond, J.M. and Grant, B., 1985b, Chemistry of submarine hydrothermal solutions at Guaymas Basin, Gulf of California: Geochimica et Cosmochimica

Acta, v. 49, p. 2221-2237.

Von Stackelberg, Ulrich, and von Rad, Ulrich, eds., 1990, Geological evolution and hydrothermal activity in the Lau and North Fiji Basins, Southwest Pacific Ocean: results of *Sonne* cruise SO-35: Geologisches Jahrbuch, Ad Heft 92, 660 p.

Wakita, K., and Sumii, T., 1992, Geologic background, *in* Explanatory notes for the energy-resources map of the circum-Pacific region, northwest quadrant: U.S. Geological Survey Circum-Pacific Map Series Map CP-40, p.2-3.

Wang, X., 1985, Geochemistry and genesis of postmigmatization reformed gold deposits in China: Scientia Sinica, series B, v. 27, p. 837-851.

Wang, Y., 1986, Characteristics of lead-zinc ore deposits in China and their metallogenic provinces, *in* Principal base metal deposits and their metallogeny in China, Chinese Environmental Sci. Publ. Co., p. 1-48.

Watanabe, T., Yui, S., and Xato, A., 1970, Bedded manganese deposits in Japan, a review, *in* Tatsumi, T., ed., Volcanism and ore genesis: Tokyo, University of Tokyo Press, p. 119-142.

Weiss, R.F., and others, 1977, Hydrothermal plumes in the Galapagos Rift: Nature, v. 267, p. 600-603.

Yan, Xingzhou, 1982, Geology and mineral resources of Yunnan Province: Yunnan People's Publishing House, 204 p. (in Chinese).

Yang, S., and Miao, Y., 1986, Geological characteristics of the Chengba-Lijiagou lead-zinc deposits in Gansu Province: Mineral Deposits, China, v. 5, no. 2, p. 14-23 [In Chinese with English abstract.]

Yao, J., 1988, Ore magmatism in the ore-formation of a magmatic Cu-Ni sulfide deposits and the determination of ore magmatic periods: Chengdu Institute of Geologic and Mineral Resources, Chinese Academy of Sciences, Bulletin, no. 9, p. 53-68. [In Chinese with English abstract.]

Ye, L., Sun, S., and Chen, Q., 1984, Facies characteristics of the Chinese phosphorite deposits, *in* International Field Workshop and Seminar on Phosphorites, International Geological Correlation Programme (IGCP) symposium, Fifth, 1982: Beijing, Geology Publishing Company, p. 3-4.

Yue, X., 1985, Geology of manganese deposits in China, *in* Division of Regional Geology and Mineral Resources, Ministry of Geology and Mineral Resources, ed., Monograph of geology and manganese ore deposits in China: Geol. Publ. House, p. 1-11 [In Chinese.]

Zanin, Y.N., 1984, Phosphatic weathering crusts and associated phosphate deposits of Siberia, *in* International Field Workshop and Seminar on Phosphorites, International Geological Correlation Programme (IGCP) Symposium, Fifth, 1982: Beijing, Geology Publishing Company, p. 419-434.

Zanoria, A.S., Domingo, E.G., Bacuta, G.C., and Almeda, R.L., 1984, Geology and tectonic setting of copper and chromite deposits of the Philippines, *in* Shimazaki, Y., Geologic evolution, resources and geologic hazards: International Symposium in the Geological Survey of Japan, Report no. 263, p. 419-434.

Zenkevich, N.L., 1970, Atlas fotografii dna Tikhogo Okeana: Moskva, Izd-vo Nauka, 134 p.

Zhamsran, M., Sotonikov, V.I., Berzina, A.P., Garamzhav, D., and Saryanov, Y.A., 1986, Elements determining the geological-structural model of the Erdenetuin-Obo copper-molybdenum ore field, Mongolia, *in* Friedrich, G.H., and others, eds., Geology and metallogeny of copper deposits: Berlin, Springer-Verlag, p. 271-279.

Zhang, P., 1987, Industrial minerals and rocks in China: Beijing, Geology Publishing Company, v. 2, 415 p. [In Chinese.]

Zhang, Z.M., Liou, J.G., and Coleman, R.G., 1984, An outline of the plate tectonics of China: Geol. Soc. Am. Bull., v. 95, p. 295-312.

Zhao, Y., Lin, W., Bi, C., Li, D., and Jiang, C., 1990, Skarn deposits of China: Beijing, Geology Publishing Company, 364 p. [In Chinese with English abstract.]

Zhu, G. and Li, X., 1986, Early Proterozoic stratiform magnesite-talc-jadeite deposits, *in* Zhang, Q., Early crust and mineral deposits of Liaodong Peninsula: Beijing, Geology Publishing Company, p. 424-450. [In Chinese with English abstract.]

Table 1.—Large-sized and remarkable deposits in the Northwest Quadrant.

Name	Latitude	Longitude	Type	Age of Mineralization	Commodity
RUSSIA					
Agyndja	65°15'N	148°05'E	-	-	Cu
Aikhal, Yubileinaya	66°00'N	110°45'E	Magmatic	-	Diamond
Balei	51°25'N	116°25'E	Vein	Cretaceous	Au
Darasum	52°00'N	115°00'E	Vein	-	Au
Deputatskoe	69°25'N	140°05'E	Vein	-	Sn
Dukat	62°35'N	155°10'E	Vein	Late Cretaceous	AgAu
Ebelyakhskoe	71°05'N	115°00'E	Placer	-	Diamond
Istakhskoe	69°45'N	141°40'E	Vein	-	Sn
Iultin	67°50'N	178°45'E	Vein	-	SnW
Kholodnimskoe	56°15'N	109°50'E	Vein	-	ZnPb
Korushnova	56°35'N	104°30'E	Skarn	Early Paleozoic	Fe
Krasnoyarova	56°25'N	102°30'E	Skarn	Early Paleozoic	Fe
Kukenei	69°10'N	174°05'E	Vein	Late Cretaceous	SnAg
Kunarev	63°25'N	150°55'E	Skarn	-	PbZn
Maiskoe	69°00'N	173°45'E	Vein	-	Au
Mir-Sputnik	62°30'N	113°50'E	Magmatic	-	Diamond
Natalka	61°40'N	147°40'E	Vein	-	Au
Nepa	59°25'N	107°50'E	Stratabound	Early Paleozoic	KCl
Neryunda	58°45'N	104°00'E	Skarn	Triassic	Fe
Nikolayevsk	44°20'N	135°35'E	Skarn/Vein	Neogene	PbZn
Olyutor	60°35'N	167°50'E	Vein	-	HgSb
Peshanka	66°35'N	164°30'E	Porphyry	Jurassic	CuMo
Pyrkakai	69°35'N	171°50'E	Porphyry	Late Cretaceous	SnW
Sherlovogorskoe	50°35'N	116°30'E	Vein	Triassic	Sn
Shkolnoe	61°30'N	148°50'E	Vein	-	Au
Skarn	63°30'N	158°30'E	Skarn	Late Paleozoic	Fe
Starskii	49°05'N	131°15'E	Sedimentary	-	Fe
Svetloe	62°50'N	148°00'E	Placer	Quaternary	Au
Tamvatney	63°30'N	174°15'E	Vein	-	HgW
Udachanaya	66°25'N	111°50'E	Magmatic	-	Diamond
Udarnyi	71°55'N	112°10'E	Magmatic	-	Diamond
Udokan	56°40'N	118°15'E	Sedimentary	Precambrian	Cu
Urultun	63°40'N	148°40'E	Stratabound	-	PbZn
Valkumei	69°40'N	170°10'E	Vein	Late Cretaceous	Sn
Vechernee	63°30'N	158°50'E	Porphyry	Late Paleozoic	MoCu
Vostok	46°40'N	136°00'E	Vein	Cretaceous	W
MONGOLIA					
Erdenet	49°10'N	104°15'E	Porphyry	Triassic	CuMo
Khubusgul	50°35'N	101°00'E	Sedimentary	Early Paleozoic	P
Tsagaan-Suvrag	43°45'N	108°40'E	Porphyry	Late Paleozoic	CuMo
Tumurtin Ovoo	47°00'N	113°15'E	Skarn	Triassic	Zn
CHINA					
Anshan	41°30'N	122°50'E	Sedimentary	Precambrian	Fe
Badaguan	49°40'N	119°05'E	Porphyry	Late Paleozoic	CuMo
Baiyinchang	37°00'N	104°15'E	Stratabound	Early Paleozoic	CuPbZn
Baiyun Obo	41°50'N	110°00'E	Magmatic	Precambrian	REE
Baiyun Obo	41°50'N	110°00'E	Magmatic	Precambrian	Fe
Benxi	41°30'N	123°40'E	Sedimentary	Late Paleozoic	Al

Table 1.—Large-sized and remarkable deposits in the Northwest Quadrant–Continued.

Name	Latitude	Longitude	Type	Age of Mineralization	Commodity
CHINA -continued					
Benyifu	41°30'N	123°10'E	Sedimentary	Precambrian	Fe
Changba	34°05'N	105°20'E	Stratabound	Late Paleozoic	PbZn
Chengmenshan	29°45'N	115°45'E	Porphyry/Skarn	Early Cretaceous	CuMo
Dachang	25°00'N	107°25'E	Vein	Cretaceous	SnZnPb
Dachishan	24°45'N	114°30'E	Vein	Early Cretaceous	W
Damingshan	23°36'N	108°22'E	Vein	Jurassic-Cretaceous	W
Dangping	25°30'N	114°30'E	Vein	Jurassic-Cretaceous	W
Dashiqiao	40°50'N	122°20'E	Sedimentary	Precambrian	Mg
Daye	30°00'N	114°50'E	Skarn	Early Cretaceous	CuFe
Dexing	29°20'N	117°40'E	Porphyry	Early Cretaceous	CuMo
Dianzhong area	24°45'N	102°00'E	Stratabound	Precambrian	Cu
Duobaoshan	50°15'N	125°40'E	Porphyry	Late Paleozoic	CuMo
Fankou	25°00'N	113°40'E	Stratabound	Late Paleozoic	PbZn
Gejiu	23°15'N	103°10'E	Skarn	Cretaceous	SnW
Guimeishan	24°55'N	115°00'E	Vein	Jurassic-Cretaceous	W
Haicheng	41°00'N	122°40'E	Sedimentary	Precambrian	Mg
Hongge	26°30'N	101°45'E	Magmatic	Precambrian	FeTiV
Hongqiling	43°00'N	126°35'E	Magmatic	Late Paleozoic	NiCu
Hongtoushan	42°15'N	124°30'E	Magmatic	Late Paleozoic	CuPbZn
Huangshaping	25°30'N	112°40'E	Skarn	Cretaceous	ZnPb
Huize	26°40'N	103°40'E	Stratabound	Late Paleozoic	PbZn
Jiaozuo	35°30'N	113°25'E	Sedimentary	Late Paleozoic	Al
Jinchuan	38°40'N	102°20'E	Magmatic	Early Paleozoic	NiCu
Jinduicheng	34°20'N	109°55'E	Porphyry	Early Cretaceous	Mo
Jinguashi	25°00'N	121°45'E	Vein	Neogene	AuAg
Laiyuan	39°30'N	114°35'E	Skarn	Cretaceous	CuMo
Lijiagou	33°45'N	105°40'E	Stratabound	Late Paleozoic	PbZn
Melasongduo	31°10'N	98°09'E	Porphyry	Paleogene	CuMo
Nannihu	33°55'N	111°35'E	Porphyry	Early Cretaceous	Mo
Niuxintal	41°20'N	124°20'E	Sedimentary	Late Paleozoic	Al
Panzhihua	26°30'N	101°30'E	Magmatic	Precambrian	FeTiV
Pinggui	24°45'N	110°40'E	Vein	Cretaceous	SnWZn
Pingguo-Taiping	23°45'N	107°30'E	Sedimentary		Al
Shinang	34°50'N	112°10'E	Sedimentary	Late Paleozoic	Al
Shizhuyuan	25°40'N	113°00'E	Skarn	Early Cretaceous	WSnMo
Shuikoushan	27°00'N	112°15'E	Skarn	Cretaceous	PbZn
Taolin	29°15'N	113°20'E	Skarn	Early Cretaceous	PbZn
Tongchuan area	26°15'N	103°00'E	Stratabound	Precambrian	Cu
Tonglian	30°55'N	118°00'E	Skarn	Early Cretaceous	Cu
Tongshankou	29°55'N	114°40'E	Skarn	Early Cretaceous	Cu
Wanshan	27°45'N	109°10'E	Stratabound	Cretaceous	Hg
Xianghualing	25°15'N	112°45'E	Skarn	Cretaceous	SnWZnPb
Xiaoyi	37°25'N	112°00'E	Sedimentary	Late Paleozoic	Al
Xihuashan	25°50'N	114°20'E	Vein	Early Cretaceous	W
Xikuangshan	28°00'N	111°30'E	Stratabound	Early Cretaceous	Sb
Xitieshan	37°25'N	95°55'E	Stratabound	Early Paleozoic	PbZn
Yangjiazhangzi	40°50'N	120°30'E	Skarn	Cretaceous	Mo
Yuanquan	37°50'N	113°40'E	Sedimentary	Late Paleozoic	Al
Yulong	31°30'N	97°59'E	Porphyry	Paleogene	CuMo
Zhongtiaoshan	35°25'N	111°40'E	Porphyry	Precambrian	Cu
Zibo	36°40'N	118°25'E	Sedimentary	Late Paleozoic	Al
Zunyi area	27°25'N	106°55'E	Sedimentary	Late Paleozoic	Mn

Table 1.—Large-sized and remarkable deposits in the Northwest Quadrant–Continued.

Name	Latitude	Longitude	Type	Age of Mineralization	Commodity
NORTH KOREA					
Buyeon	41°10'N	129°10'E	Stratabound	Cretaceous	Mg
Geomdeog	40°55'N	128°50'E	Stratabound	Jurassic	Mg
Hagnam	40°40'N	129°05'E	Stratabound	Cretaceous	Mg
Iweon	40°15'E	128°00'E	Stratabound	Late Paleozoic	Fe
Musan	42°10'N	129°10E	Skarn	Precambrian	Fe
SOUTH KOREA					
Sangdong	37°10'N	128°55'E	Skarn	Cretaceous	W
Geumseong	37°00'N	128°30'E	Skarn	Jurassic	Mo
Yeonhwa	37°05'N	129°00'E	Skarn	Cretaceous	PbZn
JAPAN					
Akenobe	35°15'N	134°45'E	Vein	Cretaceous	CuPbZn
Besshi	33°30'N	132°50'E	Stratabound	Late Paleozoic	CuFeS
Chichibu	36°00'N	138°50'E	Skarn	Neogene	CuZnPb
Hanaoka	40°20'N	140°30'E	Stratabound	Neogene	PbZnCu
Hishikari	32°45'N	130°00'E	Vein	Quaternary	Au
Ikuno	35°05'N	134°55'E	Vein	Cretaceous	CuPbZn
Kamaishi	39°25'N	141°50'E	Skarn	Cretaceous	FeCu
Kamioka	36°20'N	137°30'E	Skarn	Cretaceous	ZnPb
Kosaka	40°20'N	140°35'E	Stratabound	Neogene	ZnPbCu
Matsuo	39°45'N	141°00'E	Exhalite	Quaternary	SFeS
Nakatatsu	35°50'N	136°35'E	Skarn	Jurassic	ZnPb
Shakanai	40°18'N	140°25'E	Stratabound	Neogene	ZnPbAg
Toyoha	42°50'N	141°10'E	Vein	Quaternary	PbZnAg
Wanibuchi	35°15'N	132°45'E	Stratabound	Neogene	Gypsum
Yanahara	34°50'N	134°15'E	Stratabound	Late Paleozoic	FeS
PHILIPPINES					
Acoje	15°55'N	120°00'E	Magmatic	Paleogene	Cr
Acupan	16°20'N	120°40'E	Vein	Neogene	Au
Antamok	16°25'N	120°40'E	Vein	Neogene	Au
Atlas	10°15'N	123°40'E	Porphyry	Paleogene	CuAu
Bagakai	11°55'N	125°05'E	Stratabound	Neogene	CuZn
Barlo	16°10'N	120°15'E	Stratabound	Cretaceous	Cu
Coto	15°45'N	120°00'E	Magmatic	Paleogene	Cr
Dizon	15°00'N	120°15'E	Porphyry	Neogene	CuAu
Lepanto	16°45'N	120°50'E	Vein	Neogene	CuAu
Marcopper	13°25'N	122°00'E	Porphyry	Neogene	CuAu
Mesbate	12°20'N	123°25'E	Vein	Neogene	Au
Nonoc	10°05'N	125°30E'	Laterite	Quaternary	Ni
Rio Tuba	8°40'N	118°00'E	Laterite	Quaternary	Ni
St. Thomas	16°30'N	120°35'E	Porphyry	Neogene	CuAu
Sipalay	9°45'N	122°30'E	Porphyry	Paleogene	CuAu
Thanksgiving	16°20'N	120°35'E	Vein	Neogene	CuZnAu

Table 1.—Large-sized and remarkable deposits in the Northwest Quadrant–Continued.

Name	Latitude	Longitude	Type	Age of Mineralization	Commodity
BURMA (MYANMAR)					
Bawdwin	23°45'N	97°25'E	Stratabound	Early Paleozoic	PbZnAg
Monywa	22°10'N	94°55'E	Porphyry	Neogene	Cu
Myinmati	19°35'N	96°25'E	Vein	Late Paleozoic	W
Pa-an	17°00'N	97°50'E	Vein	Neogene	Sb
Tagaung Taung	23°40'N	96°15'E	Laterite	Quaternary	Ni
THAILAND					
Kanchanaburi area	14°40'N	98°40'E	Placer	Quaternary	Sn
Mae Lama	17°40'N	97°55'E	Vein	Jurassic	W
Mae Sod	16°30'N	98°45'E	Stratabound	Paleozoic	Zn
Phuket area	7°50'N	98°25'E	Placer	Quaternary	Sn
Ranong area	9°55'N	98°00'E	Placer	Quaternary	Sn
Song Toh	14°45'N	99°00'E	Stratabound	Late Paleozoic	PbZn
Takua Pa area I	8°30'N	98°30'E	Placer	Quaternary	Sn
Takua Pa area II	8°25'N	98°25'E	Placer	Quaternary	Sn
VIETNAM					
Lao Cai	23°45'N	103°55'E	Sedimentary	Early Paleozoic	P
Sin Quyen	22°30'N	103°45'E	Vein	Cretaceous	CuAu
Thach Khe	18°20'N	105°55'E	Skarn	Triassic	Fe
MALAYSIA					
Beatrice	4°35'N	101°05'E	Skarn	Triassic	SnAs
Bukit Besi	4°43'N	103°08'E	Skarn	Late Paleozoic	FeSn
Kinta Valley N	4°45'N	101°05'E	Placer	Quaternary	Sn
Kinta Valley W	4°30'N	100°50'E	Placer	Quaternary	Sn
Kinta Valley S	4°25'N	101°05'E	Placer	Quaternary	Sn
Kuala Lumpur area	4°10'N	101°45'E	Placer	Quaternary	Sn
Mamut	5°55'N	116°40'E	Porphyry	Neogene	CuAu
Pelapah Kanan	1°47'N	103°46'E	Skarn	Triassic	FeSn
INDONESIA					
Bangka, Jebus	1°50'S	105°25'E	Placer	Quaternary	Sn
Bangka, Sungailiat	2°05'S	106°05'E	Placer	Quaternary	Sn
Batu Hijau	8°50'S	116°45'E	Porphyry	Neogene	CuAu
Belitung, Manggar	2°55'S	108°10'E	Placer	Quaternary	Sn
Ertsburg	4°10'S	137°55'E	Porphyry/Skarn	Neogene	CuAu
Gebe	0°05'S	129°30'E	Laterite	Quaternary	Ni
Grasberg	4°10'S	137°55'E	Porphyry	Neogene	CuAu
North Sulawesi	approx. lat 0°45'N		A group of porphyry copper deposits		Cu
Soroako	2°15'S	121°20'E	Laterite	Quaternary	Ni
Tombulilato	0°45'N	123°00'E	Porphyry	Neogene	CuAu

Table 1.—Large-sized and remarkable deposits in the Northwest Quadrant–Continued.

Name	Latitude	Longitude	Type	Age of Mineralization	Commodity
PAPUA NEW GUINEA					
Frieda	4°35'S	141°50'E	Porphyry	Neogene	CuAu
Hessen Bay	7°50'S	147°45'E	Placer	Quaternary	Cr
Lihir	3°10'S	152°45'E	Vein	Quaternary	AuAg
OK Tedi	5°15'S	141°10'E	Porphyry	Neogene	CuAu
Panguna	6°30'S	155°40'E	Porphyry	Neogene	CuAu
Pigibut	2°30'S	152°05'E	Vein	Neogene	AuAg
Porgera	5°40'S	142°50'E	Vein	Neogene	AuAg
Ramu	5°25'S	145°25'E	Laterite	Quaternary	NiCo
Wau	7°15'S	146°20'E	Vein	Neogene	AuAg
Yandera	5°45'S	145°15'E	Porphyry	Neogene	CuMo
SOLOMON ISLANDS (NEW CALEDONIA)					
Jejevo	8°05'S	159°10'E	Laterite	Quaternary	Ni
San Jorge	8°35'S	159°40'E	Laterite	Quaternary	Ni
Tataka	8°30'S	159°45'E	Laterite	Quaternary	Ni

- no data

☆ U.S. GOVERNMENT PRINTING OFFICE: 1999 — 773-051 / 20142 Region No. 8